Processing porous architectures based on LDH: Synthesis and novel applications

Yasuaki Tokudome, Vanessa Prevot, Naoki Tarutani

Processing porous architectures based on LDH: synthesis and novel applications

Yasuaki Tokudome,[1,*] Vanessa Prevot,[2,*] Naoki Tarutani[3,4]

[1] *Department of Materials Science, Osaka Metropolitan University 1-1, Gakuencho, Naka-ku, Sakai, Osaka 599-8531, Japan.*

[2] *Université Clermont Auvergne, CNRS, Institut de Chimie de Clermont-Ferrand (ICCF), 63000 Clermont-Ferrand, France.*

[3] *Department of Materials Science, Graduate School of Advanced Science and Engineering, Hiroshima University, 1-4-1 Kagamiyama, Higashi-Hiroshima, Hiroshima, 739-8527, Japan.*

[4] *Research Center for Micro-Nano Technology, Hosei University, 3-11-15 Midori-cho, Koganei, Tokyo 184-0003, Japan.*

* Correspondence to: tokudome@omu.ac.jp; vanessa.prevot@uca.fr

Abstract:

The processing of porous architectures based on Layered Double Hydroxides (LDH) is reviewed. Especially, a focus was put on porosity in nm and μm ranges that can be prepared via various post-treatments and templating techniques for the enhancement of the original properties. A challenge toward the desired porosity is control of structural ordering as well as crystal growth of LDH. The present review paper is mainly dedicated to summarizing the synthetic approaches to access the porous LDH that have found a wide range of applications such as adsorption/environment purification, catalysis, energy storage & production and bio-applications.

Keywords:

porous, LDH, layered double hydroxide, meso, macro

1. Introduction

Inorganic porous materials have been employed in a wide range of applications, including catalysis, separation, energy storage, biomedical engineering. While amorphous materials with porosity are simply used as supports to load/accommodate functional centers, constructing porous textures with functional crystals can bring about further possibilities towards advanced applications.(Brezesinski et al., 2010; Crossland et al., 2013) The introduction of porosity into LDH, as a class of functional crystalline materials, has attracted attention in this context. Original features of LDH crystals can be further enhanced by introducing unique porosity thanks to increased surface area and better molecular/ion diffusion. In principle, nano/macrostructuration of crystalline materials is harder to achieve compared to that of amorphous counterpart, due to uncontrollable crystal growth which can disturb structural ordering, and/or structural deformation upon post treatments to compensate incompletion of crystallization.(Inagaki et al., 2002) Precipitation of aggregated particles typically form rather than homogeneous gels for crystalline LDH platelets. Controlling structural ordering as well as crystal growth of LDH is key to accomplish the synthesis of porous LDH.(Prevot and Tokudome, 2017)

This review paper overviews the synthesis and applications of LDH with various types of porous architectures. First, the main synthesis methods of LDH with porous architectures are reviewed, covering diverse pore-size scales from atomic/ionic, through nanometer, to micrometer, with shapes of films, powders, and monoliths. The representative synthesis methods for the porous LDHs include (1) *Introduction of Textural porosity*, (2) *Post-treatment*, (3) *Sacrificial Templating*, (4) *Soft Templating*, (5) *Composited (supported) LDH Synthesis* **(Fig. 1)**. A primitive porous structure of crystalline materials is formed as interstices of crystal platelets, *textual porosity*. *Post-treatment*, for example, drying processes, such as spray drying and supercritical drying, are

applied to modify the particle aggregation and thereby control *textual porosity*. Toward better structural ordering of porous LDH, sophisticated templating techniques of *Sacrificial Templating* and *Soft Templating* have been developed, inspired by silica-based sol-gel chemistry. Recently, especially due to the requirement of LDH modification on electrodes, synthesis of LDH on porous conductive supports has drawn increasing attention. This type of *Porous LDH based Composites* is also closely described. Then, various applications taking advantage of these unique porous features are briefly envisaged. Special attention is paid to applications of (1) *Adsorption and environment purification*, (2) *Catalysis*, (3) *Energy storage & production*, (4) *Bio-applications.*

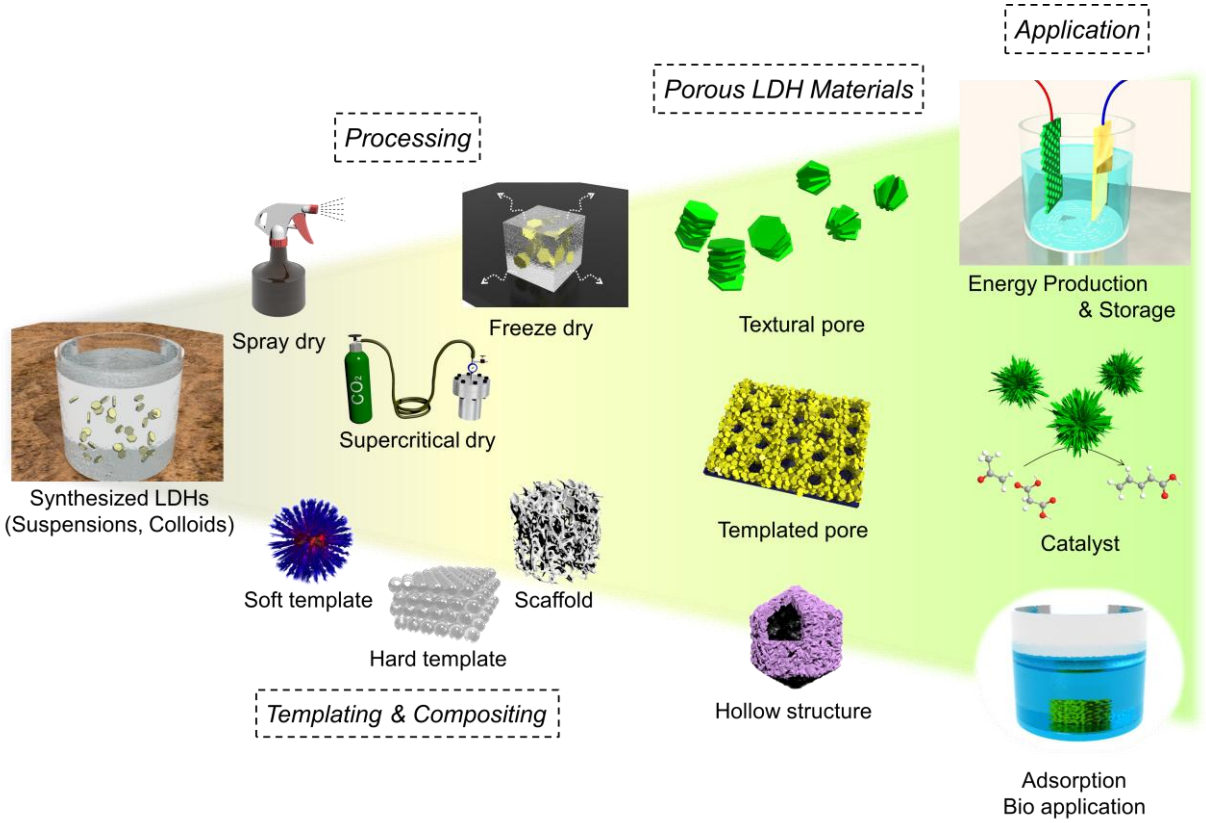

Fig. 1. Schematic illustration showing representative synthesis methods and applications of porous LDH

2. Synthesis approaches for porous LDH

2.1 Introduction of Textual porosity

Porosity in crystalline materials is often introduced as interstices of crystal platelets. Starting from metal salts dissolved in an aqueous solvent, the occurrence of crystallization accompanies with aggregation of grown crystal platelets to form porosity. This type of textual porosity is the most primitive and widely employed to achieve porous LDH materials with a large surface area. Typical conditions for the precipitation of LDH (at high ionic strength and/or at pH nearby isoelectric point) preferably form LDH aggregates with a textual porosity. The choice of alkalization agents (NaOH, Na_2CO_3, NH_4OH, urea, hexamethylenetetramine (HMT), propylene oxide (PO), glycidol) is primarily important to control the textual porosity. Co-precipitation by the addition of metal salt solutions to basic media, such as NaOH and Na_2CO_3 (Duan and Evans, 2006) and homogeneous precipitation by thermal hydrolysis of urea, known as "the urea method"(Costantino et al., 1998), are especially well-established. Textural pores obtained through the latter route tend to be larger than the one prepared with the former route due to the larger crystallite size (**Fig. 2**). The hydrolysis of urea is normally driven by heating, whereas enzymatic hydrolysis of urea is also reported as a unique scheme affording different textural properties thanks to lower reaction temperature.(Vial et al., 2006) Epoxides, such as propylene oxide and glycidol are reportedly advantageous to precipitate LDH without the inclusion atmospheric CO_2, allowing for chloride-intercalated LDH.(Oestreicher and Jobbágy, 2013) Since epoxide molecules are miscible to water and can be introduced to a reaction system at a large content, a high degree of supersaturation is achieved to allow the nanocrystallization of hydroxides.(Gash et al., 2001) Thus formed nanometric hydroxides are advantageous to prepare hierarchically porous LDHs as described in the section of *2.4 Soft-Templating*.(Tokudome et al., 2013) Additional important factors to define the textual porosity are choices of metal cations and counter anions employed for the synthesis of LDH. For example, substitution of divalent and trivalent cations in Mg-Al LDH

both influences on the textural properties of the resultant materials.(Carja et al., 2001; Triantafyllidis et al., 2010)

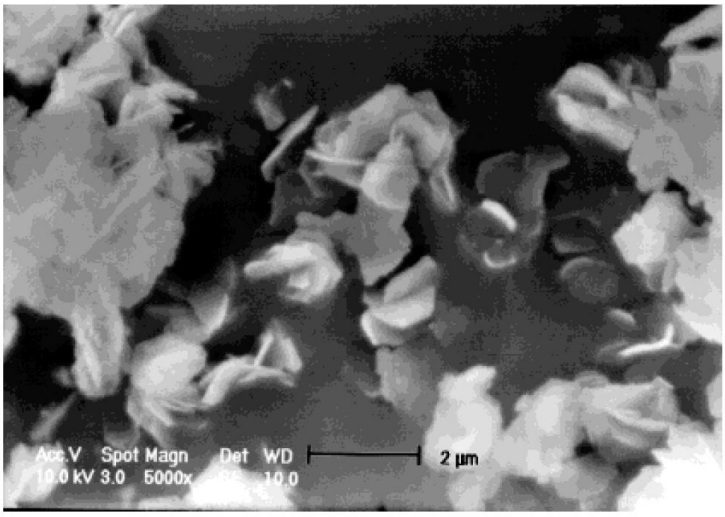

Fig. 2. A typical macroscopic texture of LDH aggregates obtained by the urea method. Reproduced from Ref. (Costantino et al., 1998) with permission from John Wiley and Sons.

Hydrothermal reaction in the presence of urea as an alkalization agent also forms LDH with unique textural porosities, where high temperature and high pressure afford to yield LDH with relatively high purity. (Li et al., 2016; Song et al., 2012; Zhou et al., 2011a) Using non-aqueous polar solvents, such as methanol, ethylene glycol, N,N-dimethylformamide (DMF), and propanol are promising options for solvothermal synthesis to yield LDH with a textural porosity.(Gunawan and Xu, 2008; Tarutani et al., 2014; Yin et al., 2018) The respective reaction steps of nucleation, crystal growth, and aggregation of crystallites can be further tuned by applying sonication(Ni et al., 2010) and/or adding chelating agents such as ethylene glycol and glycine.(Faour et al., 2012; Prevot et al., 2009) It was reported that chelating agent can impart dispersion stability of nano LDH crystals to form concentrated colloidal dispersion of LDH and layered hydroxide salts (LHS).(Tarutani et al., 2016; Tokudome et al., 2016b) The high dispersion stability allows us further nanostructuration of the formation of mesoporous structures as discussed in section *2.4*

Soft-templating. An attracting aspect of hydrothermal and solvothermal reactions is that complex reactions can be successfully designed. For example, solvothermal synthesis is favored for the synthesis of graphene-based composites because alcohols work as reductants for graphene during the crystallization of LDH.(Dreyer et al., 2011) As a more complex reaction, Kiran et al reported that a hydrothermal reaction leads to the reduction of graphene oxide and removal of silica template as well as the crystallization of LDH to form Ni-Co LDH@rGO with a textured porosity.(Karthik Kiran et al., 2019) This type of composite synthesis of LDH-based material is closely described in *2.5 Synthesis of porous LDH based Composites.*

Apart from the bottom-up techniques from metal salt solutions mentioned above, assembling exfoliated nanosheets is another promising way to form textural porosity with a higher specific surface area. A critical drawback of using exfoliated nanosheets is the occurrence of *ab*-face restacking upon solvent drying. Even though each exfoliated nanosheet presents atomic scale thickness, the restacking results in a drastic decrease of specific surface which is accessible by gas molecules. O'Hare group has developed a strategy to avoid restacking with a technique named aqueous miscible organic solvent treatment (AMOST).(Chen et al., 2015; Wang and O'hare, 2013) Where, LDH are initially prepared using a conventional coprecipitation approach but before final isolation by drying the solid is re-dispersed in an AMO solvent. This process allows to form a disordered card-house structure of LDH with a high porosity with a surface area > 350 m^2/g with remaining a high pore volume. Such exfoliated nanosheets have been used as building-units for compositing and functionalizing LDH as well as introducing porosity.(Yu et al., 2017)

2.2 Post-treatment

LDH are known to crystallize as platelet anisotropic particles and associate into a state of dense packing to form so-called stone-like aggregations. Stone-like aggregations are dense products with small pore volume as a result of face-to-face contact of platelets. Post-treatments, such as

controlled drying, recrystallization by hydrothermal and solvothermal treatments, and calcination/rehydration, are promising strategies to hinder face-to-face association and introduce porosity to the LDH-based materials (**Table1**).

Table 1. Pore characteristics of LDH -based materials after specific post-treatments.

Post-treatment	Particle size / nm	Pore diameter / nm	Specific surface area / $m^2\ g^{-1}$	Pore volume / $cm^3\ g^{-1}$	Ref
Spray drying	20−200	87.9	43	1.29	(Wang et al., 2008)
	30−100		72		(Prevot et al., 2011b)
	100−400		49−101		(Julklang et al., 2017)
		6.16	20		(Silva et al., 2019)
Freeze drying		4.08	100	0.15	(Manohara, 2014)
	61.1, 64.9 [a]		154, 137		(Moriyama et al., 2016)
	~ 30	7−19	52−97	0.11−0.28	(Liu et al., 2019)
		11.4	22		(Silva et al., 2019)
	7.1	25.6	117		(Tao et al., 2022)
	63.8	3.80	105	0.112	(Fang et al., 2022)
Supercritical drying	2−20		533−765		(Choudary et al., 2005)
	21−145		53−356	0.34−1.67	(Touati et al., 2012)
		15.5−53.2	380−502	1.40−4.27	(Tokudome et al.,

					2016a)
	~ 10	43.6	306	5.3	(Takemoto et al., 2020b)
Hydro/Solvothermal treatment	250	4−5	232		(Jia et al., 2020)
	> 15	3.97−41.7	17−300	0.24−0.35	(Song et al., 2012)
	6.8−17.7 [a]	7.3−16.8	184−415	0.42−1.24	(Tarutani et al., 2014)
	13 (thickness) > 300	6.1−12.6	46−155	0.29−0.47	(Zhang et al., 2022)
	10−15 (thickness)		70		(Wu et al., 2020b)
		3.8	230		(Liao et al., 2022)
	30 (thickness), 600	5−10	27	0.12	(Li et al., 2020a)
		21, 24	56, 53	0.28, 0.29	(Liu et al., 2022)
Calcination-rehydration	336, 419	20.7, 20.3	56, 66		(Kim et al., 2018)
	8.6−20.2 [a]		5−204		(Xu et al., 2023)
		3.3−16.4	26−112	0.03−0.33	(Barros et al., 2022)

[a] The values represent crystallite sizes

Drying process determines textural pore characteristics of LDH-based materials because as-synthesized LDH are dispersed in a reaction solution and required to be separated from the solvent. In the case of spray drying, colloids and suspensions containing LDHs are atomized into microdroplets in the drying chamber, which allow evaporation in sub-second timescale. Such a rapid evaporation prevents dense packing of building block LDH particles, which leads to the formation of relatively large textural pores. F. Zhang et al. reported to synthesis LDH microparticles

with textual porosity by spray drying.(Wang et al., 2008). The morphology, surface structures, porous structures of microparticles are controllable by changing processing conditions, such as drying temperature, gas flow rate, and sample concentration. (Julklang et al., 2017; Tarutani et al., 2019a)

Freeze drying is another approach to produce porous materials. Freezing and sublimation of the solvent (typically H_2O) of LDH dispersed solution prevent association of particles and leave macropores. Freeze drying applied to LDH materials was first reported by C. Forano et al. to prevent restacking of exfoliated LDH nanosheets.(Leroux et al., 2001) The feature of freeze dried LDH materials is a fluffy texture with discrete particles resulting from minimized surface tension.(El Hassani et al., 2019; Intasa-Ard et al., 2019; Moriyama et al., 2016) Compared with conventional thermal drying, freeze dried LDH showed expansion of basal spacing (~ 0.20 Å), which may result in the elimination of interlayer water molecules.(Moriyama et al., 2016)

Supercritical drying allows materials to dry without any surface tension, which is a promising way to avoid shrinking completely. Owing to this feature, the supercritical dried LDH materials showed significantly high specific surface area when nanocrystals are employed as building blocks. Prevot et al. first reported preparation of porous LDH materials by supercritical dying.(Touati et al., 2012) Nanoparticulate LDH with various chemical compositions were synthesized by fast precipitation and supercritical dried. Resultantly obtained aerogels showed a large specific surface area, 356 m^2/g, and a pore volume, 1.67 cm^3/g, at maximum. As another example, Tokudome and Kanamori et al. reported supercritical dried transparent LDH aerogel monolith with a high structural homogeneity showing specific surface area of 306 m^2/g by using ~ 10 nm sized LDH nanocrystals (**Fig. 3**).(Takemoto et al., 2020b) The relatively large pores (43.6 nm) are formed as a result of the formation of a network of secondary particles.

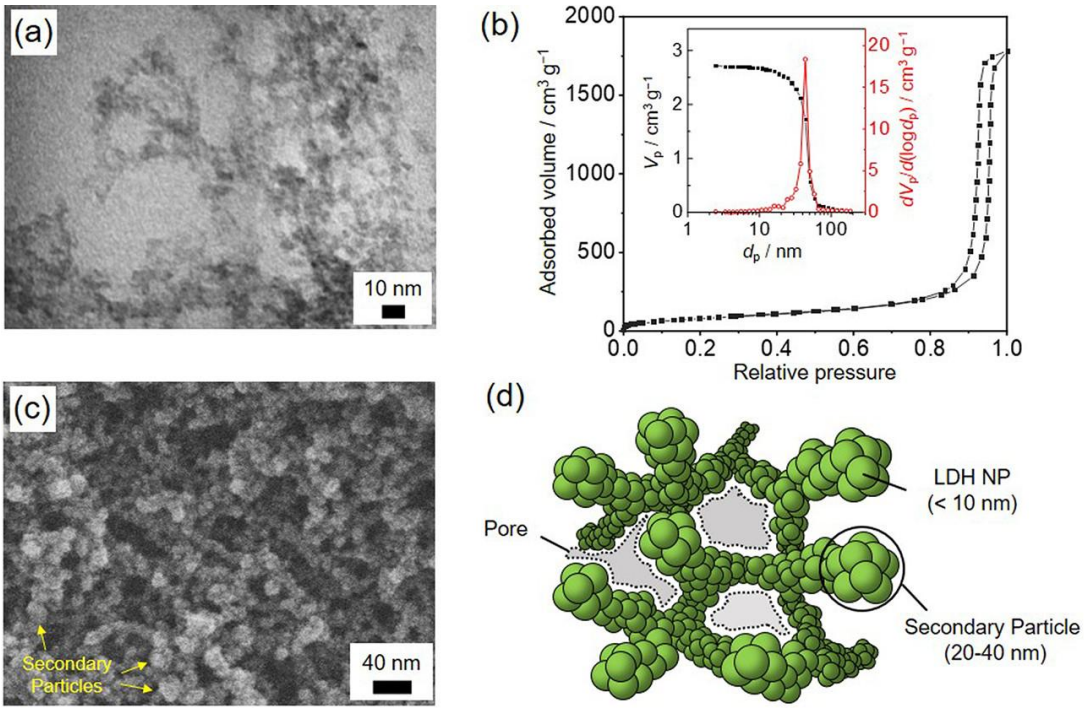

Fig. 3. a) TEM image and (b) N_2 adsorption–desorption isotherm of the Ni–Al LDH aerogel. Inset of (b) shows the cumulative pore volume (V_p) and pore size distribution ($dV_p/d(\log d_p)$) calculated by the Barrett–Joyner–Halenda method using the adsorption branch. (c) SEM image of the Ni–Al LDH aerogel monolith. (d) Schematic illustration of a solid gel network of Ni–Al LDH aerogel. Reproduced from Ref. (Takemoto et al., 2020b) with permission from ACS publications.

Hydrothermal and solvothermal treatments are employed as a post and additional step to assure better crystallization, leading to particle growth through the dissolution-recrystallization mechanism,(Song et al., 2012; Xu et al., 2006) and leaving pores as particle interstices. For example, it is reported that the crystallite size of LDHs increased from 6.8 nm to 17.7 nm after solvothermal treatment at 180 ºC, which increased mesopore size from 8.5 nm to 16.8 nm.(Tarutani et al., 2014)

Calcination and rehydration treatment is an additional effective process to introduce pores to LDH materials.(Li et al., 2005; Othman et al., 2006) It is well understood that LDH form mixed metal oxides by heat treatment at the appropriate temperatures (300−600 ºC). Dehydration, deintercalation of anions during heat treatment, lead to the deformation of the layered structure and

meso-scale pores. These pores are maintained even after rehydration and increase specific surface area of rehydrated LDH materials.(Kim et al., 2018)

2.3 Hard Sacrificial Templating

The sacrificial hard template methods have proven to be very suitable for the preparation of different kinds of hollow structured nanomaterials, promising when compared to bulk materials. In the case of LDH, two main strategies can be distinguished: i) the use of hard sacrificial templates which only play the role of support for LDH formation or deposition and are then completely removed to release the porosity and ii) the possibility of involving precursor materials which can act both as hard template to induce the LDH nanostructuring and shell formation, and as a sacrificial reservoir of precursors which is progressively consumed to form the hollow shell.

Concerning the first strategy, special attention should be given to two main aspects regarding the porous LDH synthesis, 1) firstly by exploring appropriate reaction conditions including reactants, solvent, precipitant agent, concentrations and temperature; and 2) ensuring for the resultant network of 2D LDH platelets with an appropriate rigidity to avoid the collapse of the porous LDH phase during the removal of the template. Spherical materials are frequently used as a sacrificial template; the deposition of LDH being carried out either by the self-assembly of preformed LDH nanoparticles or by *in-situ* coprecipitation on the surface. To perform the *in-situ* coprecipitation of LDH, adapted synthetic methods already reported for standard LDH synthesis (Forano et al., 2013) are carried out such as, classical coprecipitation in presence of basic agent, coprecipitation using retardant base (urea, HMT…), electrosynthesis through the nitrate reduction, or induced hydrolysis (**Table 2**). At the end of the process, the template spheres are removed according to their nature by either dissolution or combustion, resulting in an LDH porous structure. Interestingly, when the sacrificial template is removed by calcination at a moderate temperature, the derived layered mixed oxides formed can be to a certain extent regenerated in LDH structure by simple rehydration.

Uniform polymer beads, easily prepared in a wide range of sizes and commercially available, are probably the most common colloidal particles used as a hard template. Hollow capsules of LDH can be prepared using polystyrene (PS) beads (D_p = 1.3 μm) (Li et al., 2006) and the so-called layer-by-layer (LbL) assembly technique, initially developed by Decher and coworkers (Decher, 1997) to form uniform polymer films through the sequential adsorption of polyanions and polycations. In the case of LDH/PS core-shell particles, they are formed by 20 alternate depositions of exfoliated Mg-Al LDH nanosheets and poly(sodium 4-styrene sulfonate) (PSS) onto PS spheres. The self-assembly was driven by electrostatic interaction between the positively charged LDH sheets and the latex beads leading to the formation of the 3D nanostructure. Hollow LDH capsules were subsequently obtained (**Fig. 4A**) after the removal of the PS core and the PSS polyanion by controlled calcination at 500 °C and exposure to humid air. It is also possible to obtain thin-walled macroporous honecomb nanostructures of LDH or derived mixed oxides by performing a direct coprecipitation in the presence of polymer beads followed by calcination.(Pan et al., 2020; Woodford et al., 2012)

In using well-organized colloidal crystal made of PS beads, three-dimensionally ordered macroporous (3- DOM) LDH with interconnected pores were prepared by filling the voids into the array. The wetting interactions during the infiltration were key to favoring the ordered macroporous morphology.(Géraud et al., 2006; Géraud et al., 2008; Martin et al., 2016; Mostajeran et al., 2017; Prevot et al., 2011a; Tokudome et al., 2016b) Different approaches were successfully described (**Fig. 4**) to introduce LDH into voids of the array such as coprecipitation by successive impregnations, electrogeneration or infiltration of nanoparticles. It is noteworthy that the properties of such interconnected macroporous networks can be easily tuned by modifying the initial diameter and surface of the PS beads.

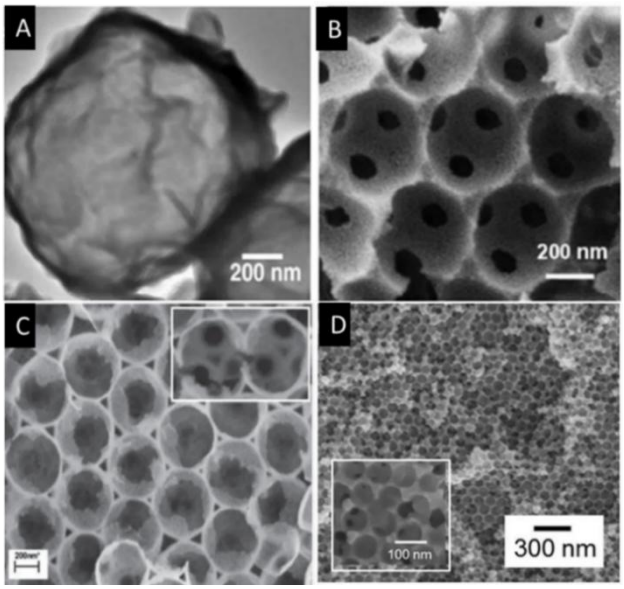

Fig. 4. Macroporous structures obtained in using polymer spheres as hard sacrificial template and A) LDH LbL deposition, B) LDH confined coprecipitation, C) LDH electrodeposition and D) LDH nanocluster infiltration. Reproduced from Ref. (Li et al., 2006; Prevot et al., 2011a) with permission from the Royal Society of Chemistry. Adapted with permission from (Géraud et al., 2008)Copyright (2016) American Chemical Society.

Monodisperse silica spheres, carbon microspheres, and hollow carbon microspheres have also been extensively used as sacrificial templates, silica being dissolved at basic pH while carbon spheres can be easily removed by calcination. Shao and co-authors reported that high alkaline conditions must be guaranteed to promote the complete dissolution of the silica core and preparation of hollow LDH microspheres. For intermediate basic conditions, LDH microspheres with various interior architectures were produced such as yolk-shell and core-shell architectures.(Shao et al., 2012) Usually, the LDH phase is associated to these sacrificial templates following similar strategies as previously described for polymer microspheres. However, in order to further promote the direct growth of LDH shell on the surface of the template, a thin layer of AlOOH can be deposited on the surface of the template which acts as a source of Al^{3+}. Moreover, silica beads have also made it possible, in the presence of resorcinol-formaldehyde and melanin, to synthesize carbon hollow microspheres enriched in nitrogen, capable of producing carbon/LDH composites exhibiting high electrochemical performance .(Xu et al., 2014)

Table 2 gathered the main hard sacrificial templates and the associated LDH deposition methods reported in the literature to prepare porous LDH phases.

Table 2 Porous LDH obtained by sacrificial templating approach.

Sacrificial template	LDH composition	Method	Removal technique	Ref
PS spheres 1.3 μm	MgAl-	Layer-by-layer	Calcination 480°C 4h	(Li et al., 2006)
PS spheres 1.0 μm	MgAl	Layer-by-layer	Dissolution in tetrahydrofuran	(Katagiri et al., 2018)
PS spheres 350 nm	MgAl-	Coprecipitation	Calcination 450°C 15h	(Woodford et al., 2012)
PS spheres 0.6-1.6 μm	CoFe-	Coprecipitation	Calcination 700°C 4h	(Zhang et al., 2010)
Hollow Polymer spheres	NiAl	Coprecipitation	Calcination 300°C 5h	(Pan et al., 2020)
PS Colloidal crystal	NiAl-	Nanoparticles infiltration	Dissolution in chloroform	(Tokudome et al., 2016b)
PS Colloidal crystal	NiAl-	Electrosynthesis	Dissolution In toluene	(Martin et al., 2016; Prevot et al., 2011a)
PS Colloidal crystal	MgAl, NiAl, CoAl, ZnAl, ZnCr, MgFeAl, MgCoAl,	Successive impregnation	Calcination 450°C 4h or dissolution in toluene	(Abolghasemi and Yousefi, 2014; Da Silva et al., 2014; Géraud et al., 2006; Géraud et al., 2008; Halma et al., 2009)
SiO_2/AlOOH	MgAl-, NiAl	Urea induced hydrolysis	Basic dissolution Urea, 100°C, 48h	(Shao et al., 2012)
SiO_2 250 nm	NiFe-CoFe-CoNi-NiAl-	*In-situ* co-precipitation	Dissolution HMT, 120°C, 24h	(Zhang et al., 2016)
SiO_2	NiCo-NiMn-	*In-situ* coprecipitation	Dissolution 0.5M KOH, 1h	(Li et al., 2017)
SiO_2/g-C_3N_4/AlOOH	NiAl-	Urea induced hydrolysis	Basic dissolution Urea, 100°C, 24h	(Shi et al., 2020a)
SiO_2/Carbon Hollow	NiAl-	Urea induced hydrolysis	Etch process, 2M NaOH , 85°C, 12h	(Xu et al., 2014)

microspheres				
Carbon microspheres	MgAl-	Nanoparticles Self-assembly	Calcination, 500°C, 3h	(Gunawan and Xu, 2009)
Carbon microsphere	ZnAl-	Nanoparticles Self-assembly	Calcination, 500°C, 3h	(Lyu et al., 2020)
Carbon microsphere	Mg_2NiAl-	Nanoparticles Self-assembly	Calcination, 450°C, 3h	(Zhang et al., 2019)

In parallel, the second strategy of hard sacrificial template mainly involves the template etching of metal-organic frameworks (MOF) to prepare 3D non-spherical LDH hollow structures of great interest for applications in energy storage and conversion. MOF are crystalline materials, constructed from a variety of metal centers and polydentate organic ligands. In this strategy, MOFs act as both support and metal cation source, mainly Co^{2+} and Zn^{2+} for the precipitation of the LDH phase shell. The general process is based on the simultaneous acidic etching of the sacrificial MOF core and hydrolysis/oxidation of metal ions leading to the precipitation of the corresponding LDH shell. Interestingly, this method is simple to carry out and the final step corresponding to the temple removal is not necessary, which prevents possible damage to the hollow structures. Zeolitic imidazolate frameworks (ZIF) were mainly involved in the preparation of various hollow LDH structures such as dodecahedral nanocages. (**Table 3**).

Table 3 Different LDH phases obtained using MOF as sacrificial template.

LDH phase	**Hollow nanostructrues**	**Sacrificial MOF**	**Conversion conditions**	**Ref**
NiCo-LDH MgCo-LDH	Rhombic dodecahedral nanocages	ZIF-67	Reflux1h in ethanol containing Mg^{2+} or Ni^{2+} nitrates	(Jiang et al., 2013)
NiCo-LDH	Nanoparticles-Nanoflakes	ZIF-8	$Ni(NO_3)_2/Co(NO_3)_2$ in methanol solution 24h then transferred into 1M NaOH	(Yu et al., 2016a)
NiCo-LDH	Rhombic dodecahedral nanocages	ZIF-67	Solvothermal treatment 120°C, 2h in ethanol containing $Ni(NO_3)_2$	(Yilmaz et al., 2017)
NiFe	Polyhedrons	MIL-88A	Ethanol/water solution containing $Ni(NO_3)_2$ and urea	(Zhang et al.,

				2018a)
NiCo-LDH	Dodecahedron	ZIF-67	Solvothermal treatment 90°C 2h in ethanol containing Ni^{2+} nitrates	(Zhou et al., 2019)
NiCo-LDH	Dodecahedron	ZIF-67	Ethanol containing $Ni(NO_3)_2$ ultrasonication 45 min	(Hu et al., 2019)
NiCo-LDH	Hollow nanocages in hollow sphere	ZIF-67	Solvothermal treatment 90°C 1h, in ethanol with $Ni(NO_3)_2$	(Lee et al., 2019)
NiCo-	Microsphere	$[Ni_3(OH)(Ina)_3(BCD)_{1.5}]$*	KOH 1M 6h	(Xiao et al., 2019)
	Tube	MoO3@ZIF-67	Solvothermal treatment 90°C 4h in methanol with $Ni(NO_3)_2$	(Chen et al., 2020)
Fe-Co-Ni LDH	Nanocages	ZIF-67	Solvothermal treatment 80°C 1h in ethanol containing Fe^{3+} and Ni^{2+} nitrates	(Zhang et al., 2020c)
NiFe-LDH	Flowerlike	MIL-100	$Ni(NO_3)_2$ in water with urea, hydrothermal treatment 120°C, 12h	(Shi et al., 2020b)

*BDC 1,4- benzenedicarboxylate; Ina : isonoctinate

Typically, the NiCo LDH phase is formed through the gradual etching of ZIF-67, possible partial oxidation of the Co^{2+}, hydrolysis of the metal nitrate in solution and subsequent coprecipitation of Ni^{2+} with Co^{2+}/Co^{3+}. Thanks to an intermediate pyrolysis step at 400°C of the ZIF-67 and sulfurization of the C/LDH formed, NiCo-LDH/Co_9S_8 hollow structure was constructed as shown in **Fig. 5**. retaining the original shape of the sacrificial template. CoNi-LDH hollow porous structures can also be used to generate CoP and Ni_2P nanoheterostructures implanted in hollow porous N-doped polyhedrons.(Yilmaz et al., 2017)

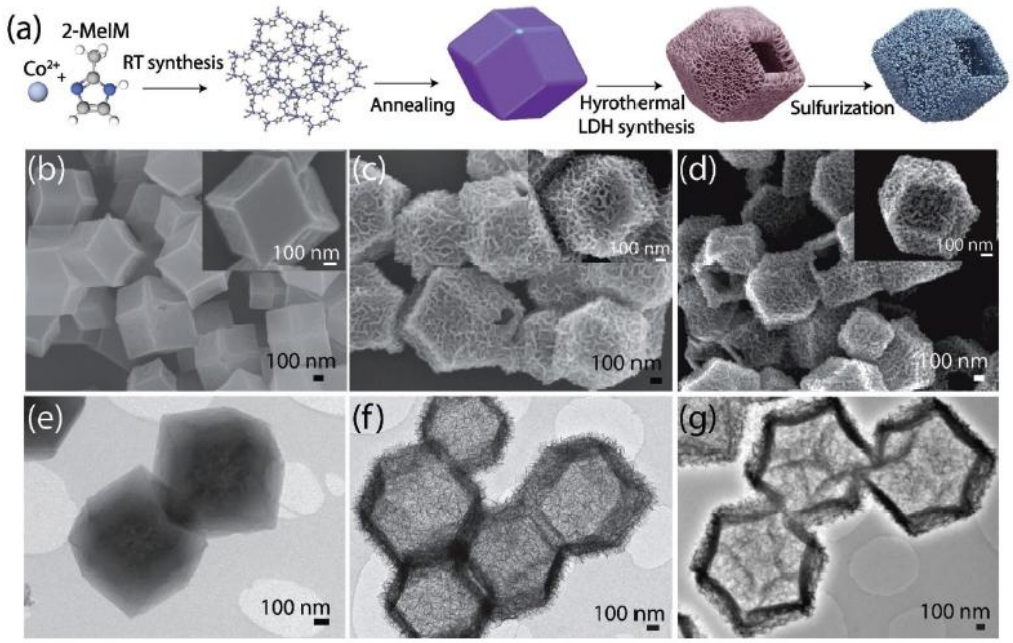

Fig. 5. Schematic illustration for the synthesis process of hollow NiCo-LDH/Co_9S_8. SEM images of b) ZIF-67-C, c) C/LDH, and d) C/LDH/S polyhedrons. TEM images of e) ZIF-67-C, f) C/LDH, and g) C/LDH/S polyhedrons. Reproduced from Ref.(Yilmaz et al., 2017) with permission from Wiley

It should be underlined that not only MOF can act as sacrificial template precursors. Following a similar approach nickel nanoprism precursor was also successfully involved in the synthesis of NiFe LDH hollow tetragonal nanoprisms coprecipitated through hydrolysis of iron(II) sulfate solution and dissolution of the inner core (Yu et al., 2018) while hollow NiFe nanospheres were synthesized via the transformation in mild hydrothermal conditions of $Ni(OH)_2$ nanospheres in presence of Fe^{3+}.(Jia et al., 2020)

2.4 Soft-templating

Kuroda and coworkers reported the synthesis of mesoporous silica with a uniform pore size distribution from layered polysilicate, Kanemite in 1990.(Yanagisawa et al., 1990) In the same year of a patent application filed, Mobil's group also reported mesoporous silica and aluminosilicate, M41S family.(Kresge et al., 1992) Since these innovative works, soft templating, especially known as liquid crystal templating, has been widely adopted to prepare mesoporous materials in alkoxide-derived sol–gel systems. Micelles of amphiphilic organic molecules (surfactants and water soluble polymers) are used to template well-defined mesoporous structures. Cooperative self-assembly of organic templates and inorganic precursors form organized architectures in mesoscale and subsequent removal of organic templates by extraction or calcination leave well-defined porous structures. The structure of the meso-phase depends on the packing properties of the surfactant molecules, and thereby the structure of mesopores obtained by soft templating is highly tunable by the nature of the surfactant and composition of the starting mixture.(Soler-Illia et al., 2002)

The synthesis of mesoporous materials with a crystalline wall, including mesoporous LDHs, is rather difficult to achieve compared to the ones with an amorphous wall. Micelles represent colloidal dispersions with a particle size normally within 5–100 nm range,(Torchilin, 2007) and therefore, inorganic crystals constructing wall of mesopores are required to be small enough in nm range. Indeed, in several oxide systems, well-ordered mesoporous structures with a crystalline wall have been demonstrated with crystals less than 4–6 nm when pluronic surfactants (poloxamers) are used as soft templates.(Chane-Ching et al., 2005; Wong et al., 2001) As well as controlling the size of crystals, the affinity between constituent inorganic particles and template, and interparticle interactions also dictate the ordering and diversity of the mesostructures.(Tang et al., 2017; Tarutani et al., 2019b) The requirement for the synthesis of LDH nanoparticles with high dispersion stability is a primal challenge toward porous LDH via soft templating.

To date, there have been many reports on the synthesis of porous LDH in the presence of surfactant molecules. Sodium dodecyl sulfate system (SDS) is widely-employed to prepare porous LDH materials. Various unique microstructures have been reported such as coral-like porous MgAl LDH microspheres,(Gunawan and Xu, 2008) flower-like MgAl porous microstructures(Sun et al., 2016; Zhang et al., 2015), MgFe LDH microspheres with hollow, yolk–shell and solid interior structures(Shao et al., 2013). Electrostatic interaction between positively-charged hydroxide sheet and SDS allows intercalation of SDS into interlayer galleries to change *d*-spacing as well as macromorphology of LDH crystals.(Sun et al., 2016; Zhang et al., 2015) It is also allowed with the aid of SDS to construct composites with graphene oxides. (Wu et al., 2015; Zhan et al., 2016) For example, Wu et al. reported porous Co-Al LDH nanosheets with a dual support system using dodecyl sulfate anions and graphene sheets as structural and conductive supports, respectively. Fast ion/electron transport, porous and integrated structure, both contribute to the improvement of electrochemical characteristics.(Wu et al., 2015)

Pore size in these porous LDH systems with using surfactant additives in most cases SDS and poloxamers (Xie et al., 2021) is far larger compared to the size of micelles, where micelles indeed influence the resultant porous structure, however, the pores are not formed as a result of transcription of micelles. For example, Xie et al. reported the synthesis of mesoporous Mg–Al–mixed metal oxide with P123 template, where an averaged pore diameter is over 20 nm. It has been reported that the organic surfactants and amphiphilic polymers rather work as capping agent, and/or initial nucleation sites(Sun et al., 2016; Zhang et al., 2015), and directing agents of self-assembly of nanocrystals to microspheres.(Gunawan and Xu, 2008) Apart from the direct crystallization of LDH with surfactant, Qin et al reported the synthesis of mesoporous CoCo LDHs by a topochemical method from soft- templated β-$Co(OH)_2$.(Qin et al., 2019) Starting from the single crystalline mesoporous β-$Co(OH)_2$, the oxidative intercalation process is triggered by bromine in acetonitrile and transformed to the CoCo LDHs with Br^- intercalated. Subsequent anion

exchange and exfoliation processes yield CoCo LDH nanomesh. The topochemical and/or pseudomorphic reaction from single metal hydroxide with defined meso/macrostructures has been also employed to prepare porous MOF as well as porous LDH.(Reboul et al., 2012) Where, the pseudomorphic replication proceeds via a rapid acid-base reaction between organic linkers and hydroxides. For example, Okada et al reported that the formation of $Cu_3(BTC)_2$ (H_3BTC = 1,3,5-benzenetricarboxylic acid)) occurs from $Cu(OH)_2$ and H_3BTC in < 1s, once the two reactants are contacted allowing for the replicated structure in a diffusion-limited manner.(Okada et al., 2014)

Two step reaction known as nanobuilding block (NBB) approach is another promising route to access crystalline mesoporous materials, where nanocrystals are first formed, dispersed in a solvent with a surfactant and subjected to soft-templating.(Chane-Ching et al., 2005) Tokudome et al reported a NBB approach to access to mesoporous LDH using a nonionic surfactant (Pluronic F127) from a concentrated colloidal suspension of NiAl LDH nanoparticles with a diameter as small as 8 nm (**Fig. 6**).(Tokudome et al., 2016b) The formation of colloidal suspension of the nanometric LDH involves the transient gelation followed by the deflocculation, which simultaneously achieves nanocrystallization and dispersion under highly supersaturated conditions. The addition of acetylacetone (acac) and the amphoteric nature of aluminum hydroxide play critical roles in the reaction. The successful synthesis of

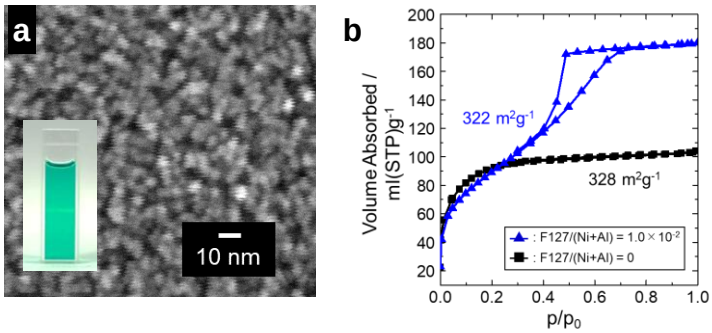

Fig. 6. (a) photograph and SEM images of NiAl LDH nanoparticles, (b) (c) N_2 adsorption-desorption isotherms of casted film samples prepared from suspensions of LDH nanoparticles with and without Pluronic F127. Reproduced from Ref. (Tokudome et al., 2016b)

with permission from American Chemical Society.

pure LDH suspended in a solvent at as high as ~100 g/L is achieved in the compositional range of $0.75 \leq acac/Al < 1.5$. The increased pore volume on the N_2 adsorption isotherm demonstrates the formation of mesopores via soft templating with Pluronic F127 (**Fig. 6b**). Another excellent example is demonstrated by Oka et al. on Mg-Al LDH with ordered mesostructures from Pluronic F127 and monodispersed Mg-Al LDH nanoparticles with 10 nm using tris(hydroxymethyl)aminomethane (THAM) as a surface stabilizing agent (**Fig. 7**).(Oka et al., 2017) The sizes of LDH can be tuned from 12 to 60 nm by changing the concentration of THAM used as a surface stabilizing agent. The successful introduction of mesopores is confirmed by the comparison of N_2 isotherms of samples with and without Pluronic F127. The mesoporous mixed metal oxides (MMO) obtained by calcination was assessed by Knövenagel condensation of ethyl cyanoacetate with benzaldehyde, revealing that the mesoporous LDH prepared with the smallest LDH, 12 nm, exhibit the best catalytic activity.

The induction of phase separation in a gelling solution containing divalent and trivalent cations is another promising strategy to achieve (hierarchically) porous LDH (**Fig. 8**). The porous LDH possess macropores in μm range as a result of phase separation (**Fig. 8a**) and mesopores as interstices of primary particles (**Fig. 8b**). The primary particles are nanometric LDH with $Al(OH)_3$ impurity (**Figs. 8c and d**).

The reaction occurs as follows : starting from an aqueous mixture of metal salts, homogeneous alkalization reaction induced by propylene oxide form embryonic poorly-crystallized LDH, leading to phase-separation into LDH-based solid phase and soluble polymer contained liquid phase.(Tokudome et al., 2007) Ambient drying or supercritical drying to remove the solvent phase leads to successful formation of hierarchically porous monolith. The monolithic LDH materials with hierarchical pores in μm and nm ranges have been reported for various systems of Mg-Al,

Mn-Al, Ni-Al, Ni-Al, Fe-Al, Co-Al. (Tarutani et al., 2015; Tarutani et al., 2014; Tokudome et al., 2013)

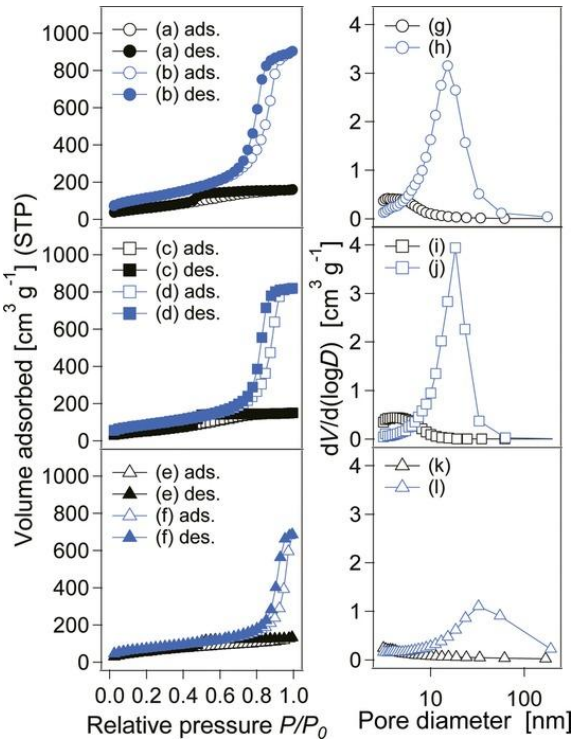

Fig. 7. (a)–(f) N_2 adsorption–desorption isotherms and (g)–(k) BJH pore size distribution curves of (a, g) MMO(12), (b, h) MMO(12)- F127, (c, i) MMO(26), (d, j) MMO(26)- F127, (e, k) MMO(60), and (f, l) MMO(60)- F127. MMO(xx): Mg–Al mixed metal oxides prepared from MgAl LDH with an average diameter of xx nm. Reproduced from Ref. (Oka et al., 2017) with permission from John Wiley and Sons.

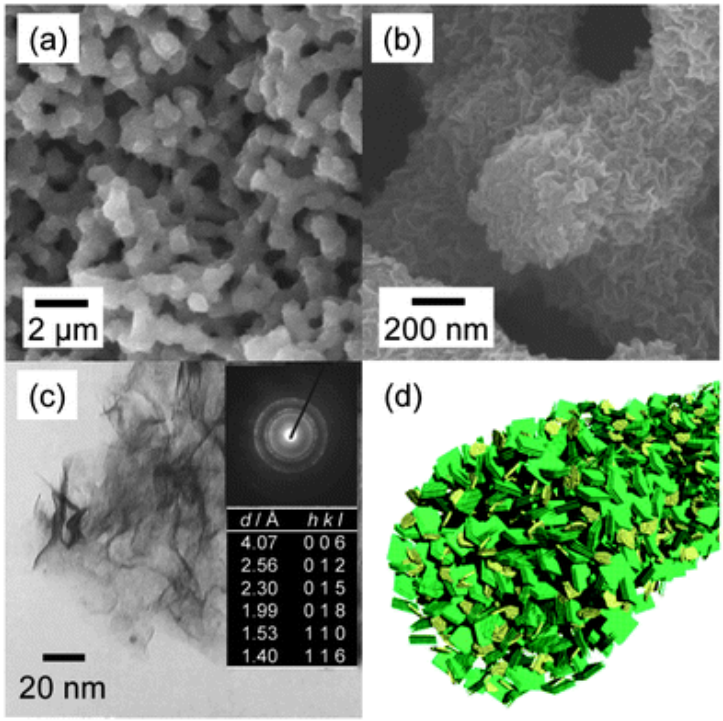

Fig. 8. (a and b) FE-SEM (c) TEM images of hierarchically-porous MgAl LDH xerogel. The inset of (c) shows an electron diffraction pattern and the corresponding assignment. (d) Schematic illustration of agglomeration state of primary particles: green: LDH crystals; yellow: aluminum hydroxide. Reproduced from Ref. (Tokudome et al., 2013) with permission from The Royal Society of Chemistry.

2.5 Porous LDH based Composites

The assembly of materials possessing complementary properties is a powerful approach to create materials with new functionalities that cannot be represented by single-phase materials. Although mixtures of LDH with many types of nanomaterials (such as oxide microspheres (Al_2O_3, Fe_2O_3, Fe_3O_4, MnO_2…), nanowires (CuO, Al, Ag), 2D layer systems (graphene, MXene…) which may bring additional functionalities to the heterostructures, are of current interest in the scientific community,(Gu et al., 2015) this will not be discussed here. Only the case of macro/meso /microporous materials will be detailed (**Table 4**). A well-developed strategy to enhance the LDH performance in many applications requires their association with a 3D porous support allowing to enhance especially the interparticle diffusion and the mass transport. The assemblies between LDH

nanoparticles and porous supports can be carried out either, by electrostatic interactions between the support and the positively charged LDH layers or, by *in-situ* coprecipitation of LDH over the surface. To promote the adhesion or the growth of LDH nanoparticles to the external surface of the porous support, a good compatibility in terms of charge and hydrophilicity must be ensured, requiring in certain cases a preliminary step of modification/activation of the support surface. For instance, carbon nanofibers were immersed in concentrated sulfuric acid before LDH *in-situ* coprecipitation to increase their hydrophilicity.(Lai et al., 2015) Since the surface of the support can also serve as a source of metal cation by partial hydrolysis for the LDH formation (*vide supra*), one way to prone oriented crystal growth of LDH on the outer surface is to modify the support surface by depositing a thin layer of reactive materials such as AlOOH.(Han et al., 2018)

When the LDH based composite is synthesized, following similar strategies as previously described for sacrificial hard template, special attention should be paid to the localization and uniform distribution of the LDH phases within the porous supports. Since multiphase materials are obtained, the structural characterization and purity of the formed LDH phases are usually difficult to put in evidence and deep characterization techniques are requested to get better insight on the materials. **Table 4** summarizes the main kinds of porous inorganic and polymer materials used to support or confine LDH particles. Obviously, a large variety of supports were reported including macro/mesoporous alumina and silica, meso/microporous materials such as zeolites, MOF, sepiolite and vermiculite, but also porous carbonaceous materials including carbon nanotubes, 3D carbon foam or aerogel, carbon fibers, and hierarchical carbon are obtained by biotempate calcination (**Fig. 9**).

For exemple, Xue et al.(Xue et al., 2018) used porous anodic aluminum oxide (AAO) acting both as a substrate and as a source of Al^{3+} to prepare 3-D NiAl LDH membrane by an *in-situ* growth technique, leading to the formation of uniform coverage of the template surface with perpendicular orientated LDH platelets. Ordered mesoporous silica can also be used as template to

produce core shell silica@LDH composite displaying a hierarchical structure as evidence on **Figs. 9 c and d**. LDH were for example coprecipitated *in-situ* on mesporous silica particles, even without any pretreatment. When an aqueous miscible organic solvent treatment (AMOST) is associated to this template synthesis to avoid aggregation of primary LDH platelets, the LDH based composite exhibited a high surface area (S_{BET}= 897 m^2/g and V_p= 0.91 cm^3/g^{-1}).(Suo et al., 2019)

Concerning the metallic foams, they were extensively used as conductive template to develop LDH supported materials of great interest for electrocatalysis for instance. The 3D macroporous metallic foam coated by LDH allows to prepare free-standing electrode promoting diffusion to the surface and leading to highly exposed active site. Yu et al. (Yu et al., 2019) reported a hierarchical 3D electrode designed by electrodeposition of NiFe- LDH nanolayers on a 3D MXene/Nickel foam frame which can boost both OER and HER in alkaline conditions (see above) (**Figs. 9 e-f**). The addition of MXene into the structure, displaying high conductivity and interesting reactive and hydrophilic properties, allowed to enhance the charge transfer kinetics and the water molecule activation.

Previously, we discussed the possibility of using MOF as sacrificial templates to produce hollow LDH phases. An alternative strategy consists in associating the two materials in a micro-mesoporous heterostructures. A ZIF-67@Co LDH yolk-shell composite was successfully prepared (**Figs. 9 g-h**) in a one-pot process by the successive increase of cobalt concentration in the methanolic solution containing also the 2-methylimidazole used as the ZIF organic ligand.(Chen et al., 2019) The use of a high molar ratio of Co^{2+}/2-methylimidazole favored the formation of Co based LDH. Such tendency can be explained due to a slight difference in thermodynamic stability between the Co-based LDH and the ZIF-67. Interestingly, the mesoporous LDH shell allowed to stabilize the ZIF-67 and its high permeability was favorable for the transport of various species.

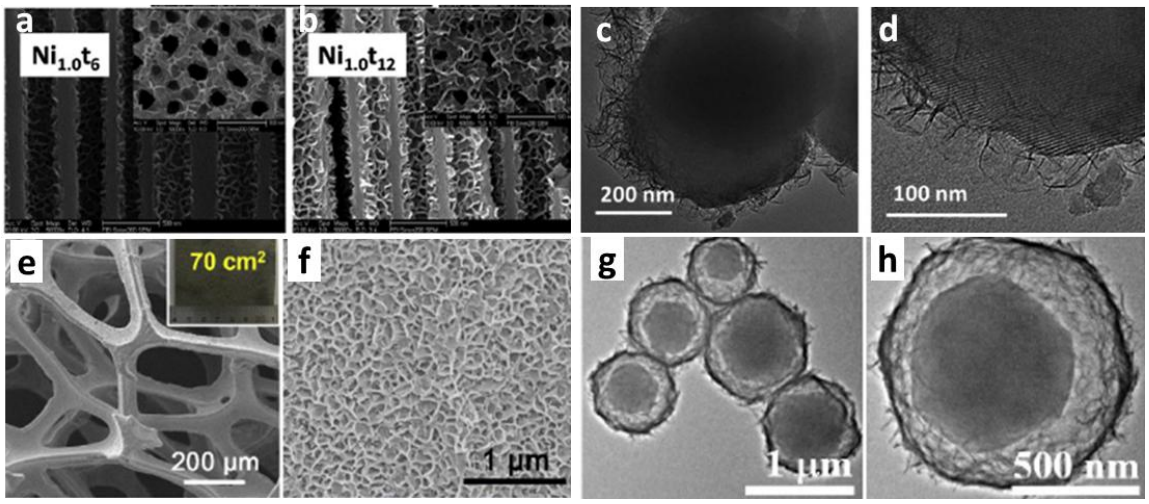

Fig. 9. SEM and TEM images of porous LDH composites prepared using (a, b) Anodic Aluminum Oxide after 6h and 12h respectively (c, d) Mesoporous ordered silica, (e, f) nickel foam and (g, h) a cobalt zeolite imidazolate frameworks (ZIF-67) Adapted with permission from (Xue et al., 2018);(Suo et al., 2019); (Chen et al., 2019) with permission from the Royal Society of Chemistry. Reprinted from (Chen et al., 2019), Copyright (2019), with permission from Elsevier.

Moreover, the unique characteristics of polymers and biopolymers facilitate the design of numerous porous polymer structures capable of interacting/incorporating LDH nanoparticles into porous nanocomposite frameworks, such as hydrogels, foams, and mats of fibers (**Table 4** and **Fig. 10**). This type of porous hierarchical nanocomposites is of great interest for the development of biomaterials and for applications in biomedicine, which will be detailed later in this chapter (*3.4 Bio-applications*).

In parallel, as many natural materials such as vegetables, fruits, and biomacromolecules (cellulose, collagen…) present interesting hierarchical morphologies, they have been deeply studied as supports for developing biotemplate-assisted synthesis approaches generally easy to implement, cost-effective and environmentally friendly. Depending on the intended application, the biotemplate can also act as a carbon source to produce a unique hierarchical carbonaceous support at a preliminary step of carbonization. LDH can then be deposited or coprecipitated at the surface of the porous polymer or biotemplate.

Carbon nanofiber membranes can be obtained from electrospun polyacrilonitrile subsequently submitted to pre-oxidation and carbonization in a nitrogen flow. As illustrated in **Fig. 10a**, such a template allowed the preparation, by one-step solution deposition method, of a hierarchical structure of carbon nanofiber@NiCo LDH hybrid membrane. By using two different kinds of growth agents, such as urea and hexamethylenetetramine (HMT), it was possible to adjust the morphology of the Ni-Co phases either into nanosheehs or nanorods.(Lai et al., 2015) CoAl-LDH particles were also *in-situ* coprecipiated from divalent and trivalent metal sulfates and urea under hydrothermal treatment at 110°C, at the surface of a poly(melamine formaldehyde) sponge. In this latter example, SiO_2 nanofibers were also present in the materials acting as pore size regulators. Modification of the surface was necessary not only to promote the growing of LDH particles but also to enhance the adhesion between the polymer sponge surface and the inorganic coating. (**Fig. 10b**) (Lv et al., 2017)

Interestingly the 3D porous nanocomposites can also be directly shaped from an LDH suspension containing the polymer in an adequate solvent. By this approach, MgAl-LDH based nanocomposite fibers involving polycaprolactone or polylactide were electrospun(Miao et al., 2012) from mixed solvent THF/DMF containing solid content, leading to a uniform dispersion of the LDH nanoparticles throughout the nanocomposite fibers as evidenced on the TEM image (**Fig. 10c**).

Considering hydrogels containing LDH, they can be easily produced as many types of porous nanocomposites; the main aspect is to obtain well-dispersed LDH particles in order to achieve nanocomposites with improved performances. In the case of a thermoresponsive poly(*N*-isopropylacrylamide) hydrogels,(Zhang et al., 2018b) the nanocomposites were synthesized by *in-situ* free radical polymerization of monomers in water containing LDH nanoparticles (80 nm). The SEM image (**Fig. 12 d**) of the freeze-dried nanocomposite hydrogels along the vertical section exhibits a hierarchical layered porous architecture.

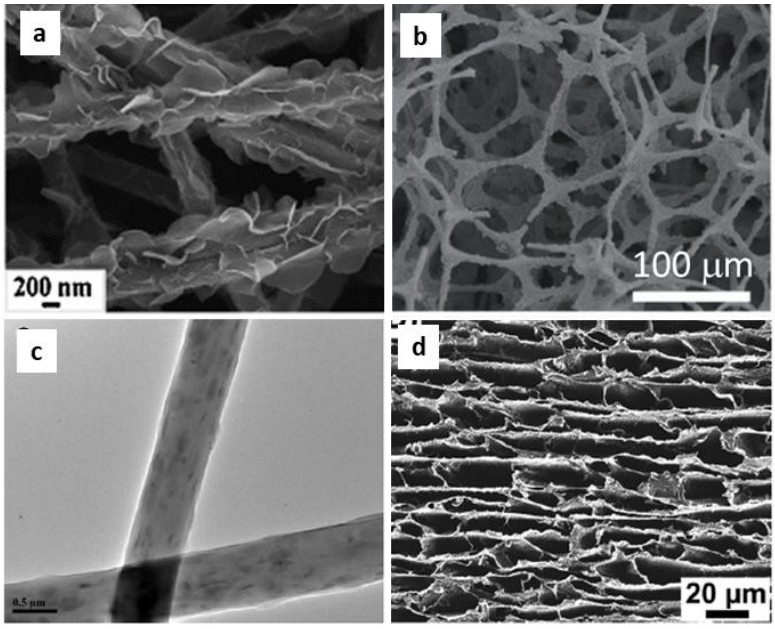

Fig. 10. SEM and TEM images of LDH nanocomposites prepared using porous polymers (a) carbon nanofibers derived from electrospun polyaniline, (b) poly(melamine formaldehyde) sponge (c) electrospun polycaprolactone and (d) poly(N-isopropylacrylamide). Adapted with permission from(Lai et al., 2015) and (Miao et al., 2012). Copyright (2015, 2012), with permission from Elsevier. Reprinted from (Lv et al., 2017), Copyright (2017), with permission from John Wiley and Sons. Adapted with permission from (Zhang et al., 2018b) with permission from the Royal Society of Chemistry.

Table 4 Various porous supports and conditions used to prepare 3D porous LDH composites

Support	**Support**	**LDH phase**	**Method**	**Conditions**	**Ref**
Porous Oxides	Biotemplated Al_2O_3	MgAl-, ZnAl-, NiAl-	Induced hydrolysis	75°C-140°C / 10h	(Zhang et al., 2014)
	θ-Al_2O_3 spheres	MgAl-	Induced hydrolysis	HT 90°C/ 24h	(Zhang et al., 2012)
	Tubular α-alumina	MgAl-	Electrophoresis	1V- 20V	(Kim et al., 2008)
	Macroporous γ–Al_2O_3	MgNiCo-	Induced hydrolysis Urea	120°C/ 24h	(Yue et al., 2015)
	Anodic Aluminum Oxide (AAO)	ZnAl-, NiAl-	Induced hydrolysis	80°C/ 12h	(Xue et al., 2018)
	Mesoporous SiO_2 coating	MgAl-	In-situ sol-gel process	RT/ 30 min	(Cao et al., 2018c)

	Mesoporous SiO_2 spheres	Co_2Al-	Alternate deposition	Formamide	(Jiang et al., 2014)
	Mesoporous SiO_2 spheres	MgAl-	*In-situ* coprecipitation	RT/ 30 min	(Suo et al., 2019)
	MCM-41	ZnCr-	*In-situ* coprecipitation	-	(Sahoo et al., 2020; Sahoo et al., 2019)
	SBA-15	CuAl-	*In-situ* coprecipitation	80°C/ 18h	(Ji et al., 2019)
	SBA-15	MgAl-	Induced hydrolysis	600°C/6h HT rehydration	(Li and Shi, 2008)
	Meso-macro Al-SBA-15	MgAl-	Induced hydrolysis	450°C/15h HT 125°C/ 21h	(Creasey et al., 2015)
	ZnO nanorod on Carbon fiber cloth	NiCo-	Electrosynthesis	50°C/ 1.5h	(Liu et al., 2017)
Metallic foams	FeCr alloy foam	NiAl-	Electrosynthesis	-0.9 V/ -1.2V 600-1800s	(Basile et al., 2008; Basile et al., 2009)
	FeCr alloy foam	MgAl-	Electrosynthesis	-1.2 V/ 2000 s	(Benito et al., 2014)
	Ni foam	NiFe-	Electrosynthesis	-1.0 V/ 300s	(Lu and Zhao, 2015)
	Ni foam	NiFe- CoFe-	Electrosynthesis	-1.0 V/ <300 s	(Li et al., 2015)
	PPy nanowire/Ni foam	NiCo-	Electrosynthesis	-1.0 V/ < 200 s	(Shao et al., 2015)
	Ni foam	NiAl-	*In-situ* coprecipitation	HT 120°C/12h	(Liu et al., 2015c)
	Ni foam	CoAl-	*In-situ* coprecipitation	HT 120°C/6h	(Guoxiang et al., 2014)
	$Co(OH)_2$/ Ni foam	CoAl-	*In-situ* coprecipitation	HT 100°C/ 24h	(Abushrenta et al., 2015)
	$Co_2(OH)_2CO_3$/Ni foam	CoFe-	*In-situ* coprecipitation	HT 100°C/ 8h	(Yang et al., 2014)
	Ni foam	NiCo-	-	180°C/ 24h	(Chen et al., 2014)
	Porous titanium	MgAl-	Deposition	37°C/ 3 days	(Badar et al., 2015)
Porous minerals	Zeolite	MgAl-	*In-situ* coprecipitation	2h/ RT	(Chen et al., 2016)
	Sepiolite	MgAl-	*In-situ* coprecipitation	4h/ RT	(Gómez-Avilés et al., 2016)
	Sepiolite	$Fe^{II}Fe^{III}$	*In-situ* coprecipitation	-	(Tian et al., 2016a)
	Vermiculite	MgAl-	*In-situ* coprecipitation	HT 120°C/ 24h	(Tian et al., 2016b)

	ZIF-8	MgAl	Seeds deposition and growth	-	(Liu et al., 2014a; Liu et al., 2014b)
	ZIF-67	$Co^{II}Co^{III}$-	*In-situ* formation	RT/24h	(Chen et al., 2019)
Porous carbons	Carbon fiber cloth	CoFe-	*In-situ* coprecipitation	HT 100°C/3h	(Ma et al., 2016)
	Carbon fibers	CoAl-	*In-situ* coprecipitation	HT 90°C/ 6h	(Zhao et al., 2013)
	Electrospun carbon nanofibers	NiCo	*In-situ* coprecipitation	80°C/ 6h	(Lai et al., 2015)
	Graphene sponge	MnNi-	*In-situ* coprecipitation	HT 90°C/6h	(Wan et al., 2015)
	MWCNT	Ni/Co Mn	*In-situ* coprecipitation	RT/24h	(Jia et al., 2016)
	GO nanocups	NiAl-	*In-situ* coprecipitation	HT 100°C/24h	(Lin et al., 2013)
	Carbon cloth	NiCo Mn-	Electrodeposition	-1.0 V/30-90s	(Cao et al., 2019)
	Carbon NP/AlOOH	NiAl	Induced hydrolysis Urea	HT 100°C/24h	(Liu et al., 2015b)
	Carbon cloth/ AlOOH	NiAl-	Induced hydrolysis	75°C/20h	(Hai and Zou, 2015)
	Activated carbon fiber cloth	Mg_3Al- Ca_3Al-	Electrophoresis	40V / 60 min	(Ma et al., 2015)
	ZIF-8 derived Carbon	NiAl-	Induced hydolysis	-	(Han et al., 2018)
	Cotton dervived carbon fibers	MgAl-	*In-situ* coprecipitation	HT 130°C/ 10h	(Sun and Chen, 2020)
Polymers	Polyurethane foam	MgAl- NiAl-	Layer-by Layer	Alginate and chitosan	(Liu et al., 2015a)
	Melamine polymer foam	NiCo-	Induced hydrolysis	Ethanol reflux 1h	(Ghani et al., 2016)
	PNIPAM/PAM	MgAl-	In-situ polymerization	25°C/ 72h	(Zhang et al., 2018b) (Hu and Chen, 2014)
	Cellulose	ZnAl-	*In-situ* coprecipitation	RT/ 24h	(Mandal and Mayadevi, 2008)
	Cellulose	ZnAl-	*In-situ* coprecipitation	100°C/ 2h	(Sobhana et al., 2016)
	Cellulose	MgAl-	*In-situ* coprecipitation	100°C/ 12h	(Yang et al., 2020a)
	Poly (ethylene glycol)	MgAl-	Mixture of aqueous suspension	-	(Huang et al., 2016)
	Alginate beads	NiAl-	*In-situ* coprecipitation	RT/ 24h	(Prevot et al., 2020)

Agarose	MgAl--	*In-situ* coprecipitation	RT/ 2-3h	(Hibino, 2020)
Agarose	NiGa-	Electric double migration	25V/ 20 min	(Gwak et al., 2017)
Chitosan	MgAl-	Mixture and lyophylisation	Acetic acid 0.1M	(Mahanta et al., 2019)
Chitosan	MgAl-	Electrodeposition	3-4 V	(Zhao et al., 2015a)
Electrospun Polycaprolactone	MgAl-	Mixture dispersed in acetone		(Romeo et al., 2007)
Electrospun Polylactide	MgAl-	Mixture dispersed in THF/DMF		(Miao et al., 2012)
Electrospun PVDF	MgAl-	*In-situ* coprecipitation	HT 120°C/24h	(Sailaja et al., 2015)
Electrospun PAN/PMMA	MgAl-	*In-situ* coprecipitation	HT 100°C/ 8h	(Shami et al., 2016)

3. Application

3.1 Adsorption and environment purification

The hydroxide layers of LDHs interact through electrostatically bonding, which is relatively weak bonding, and enables to capture organic and inorganic anions. Since LDH show excellent anion adsorption capacity, have a low toxicity for environment and human health, and are synthesized at low cost, LDH-based materials have been used in environmental application scenes such as water purification, dye removal, and CO_2 capture.(Daud et al., 2019; Goh et al., 2008; Yang et al., 2019) The introduction of porous structures enhances and maximizes the adsorption properties of LDH-based materials. Porous LDH-based materials showed excellent function in removal of harmful heavy metals, oxyanions, dye molecules, biomolecules, and CO_2 molecules (**Table 5**). These adsorbates are in solution except CO_2, therefore, improvement of diffusion by porous structures will enhance the adsorption property. It is reported that macropores (> 50 nm) enhance liquid/anion diffusion to deep inside of materials, on the other hand, mesopores (2−50 nm) increase the number of accessible sites.(Tarutani et al., 2014; Tokudome et al., 2013) In many

reports, calcined LDH are employed due to their high specific surface area. Although smaller pores are preferential for adsorption because they produce higher specific surface area in general, it is necessary to consider the size-exclusive effect of pores. For example, biomolecule (bovine serum albumin) sized as 5×7×7 nm^3 effectively adsorbed to the LDH-based materials having larger mesopore (53.2 nm) despite its smaller specific surface area. (Tokudome et al., 2016a)

There has been increasing demand for carbon capture and storage, and/or direct air capture by using LDHs in recent years because of global warming problem. LDH have been used for CO_2 sorption at high temperatures due to their advantageous characteristics; better adsorption capacity, fast kinetics, cyclic stability, and ease of preparation. Controlling nucleation and crystal growth produced LDHs with well-developed textural porosities. The textural pores remained even after thermal activation at high temperatures, which effectively enhanced CO_2 capture affinity. (Zeng et al., 2013) Synthesis of nanosized LDHs (~ 20 nm) and controlled association behavior using the isoelectric point method allows the formation of LDH materials having mesopores (18 nm) with a high specific surface area (103 m^2/g).(Wang et al., 2013) Introduced mesoporosity not only enhances CO_2 capture but also allows effective compositing with K_2CO_3 which is known to promote CO_2 capture by LDHs.

Table 5. Adsorption of heavy metals, oxyanions, dye molecules, biomolecules, and CO_2 molecules by porous LDH-based materials.

Adsorbate	Pore structure	Model	Absorption	Specific	Ref

		[a]	capacity / mg g^{-1}	surface area / m^2 g^{-1}	
As(V) Cr(VI)	Textural pore	L	216 188	225	(Yu et al., 2012)
Cr(VI)		L F	52 34	52	(Zhang et al., 2020b)
U(VI)	Hollow structure	L	557	208	(Yuan et al., 2019)
	Freeze dried	L F	764 1100 165 326	118 163	(Tao et al., 2022)
Dichromate	Textural pore	L	388	400	(Varga et al., 2021)
Phosphate	Freeze dried	L	59	105	
	Freeze dried	L	98	84	(Liu et al., 2019)
	Hollow structure	L	76 232	65 158	(Zhou et al., 2011b)
Fluoride	Textural pore	L	15	379	(Zhao et al., 2015b)
	Freeze dried	-	17 82	154 -	(Moriyama et al., 2016)
Congo red	Textural pore	L	166 273	139 123	(Jia and Liu, 2019)
	Textural pore	L	205 330	60 121	(Lei et al., 2017)
	Templated pore	L	3470	221	(Xie et al., 2021)
	Hollow structure	L	1230	133	(Huang et al., 2015)
Methyl orange	Textural pore	L	490	203	(Li et al., 2014)
	Hollow structure	L	833	127	(Lyu et al., 2020)
	Hollow structure	L	1112	164	(Xu et al., 2017)
	Textural pore	L	883	82	(Zheng et al., 2012)

Methyl blue	Hollow structure	L	398	99	(Zong et al., 2018)
Methyl orange Coomassie Brilliant blue Congo red Eosin B	Hollow structure	L	816 655 178 95	167	(Huang et al., 2017)
Congo red Methyl orange Methyl blue	Textural pore	L	1429 476 1667	204	(Zhang et al., 2020a)
Methyl orange Congo red Indigo carmine	Textural pore	L F	1052 890 513 530 527 239	27	(Li et al., 2020a)
2,4-dichlorophenol	Hollow structure	L	566	177	(Zhang et al., 2019)
Trypsin	Supercritical dried	F	1517	305	(Touati et al., 2012)
Bovine serum albumin	Supercritical dried	F	996	397	(Tokudome et al., 2016a)
CO_2	Freeze dried		1.4 mmol/g	276	(Manohara, 2014)
	Textural pore		0.24 mmol/g	133	(Wang et al., 2015)
	Textural pore		1.21 mmol/g	124	(Martunus et al., 2011)
	Textural pore		0.91 mmol/g	348	(Qin et al., 2017)
	Textural pore		0.92 mmol/g	113	(Zeng et al., 2013)
	Textural pore		0.58 mmol/g	103	(Wang et al., 2013)

[a] adsorption model; F and L are Freundlich and Langmuir model, respectively.

3.2 Catalysis

The introduction of porosity increases the specific surface area accessible by reactants and enhances the catalytic activity of original LDHs. Some of the examples of catalytic applications taking advantage of unique porous structures are summarized in **Table. 6**. The enhancement of catalytic activity has been demonstrated for photocatalysts, oxidation and hydrogenation. Reaction selectivity imparted in micro-environment and/or enhanced diffusion as well as increased surface area have been achieved by the introduction of porosity. LDH is a solid basic material and itself can work as a catalytically-active site as well as a support; even a homogeneous so-gel reaction can be induced by using dispersion of nanometric LDH.(Tokudome et al., 2022) Nevertheless, as seen in **Table 6**, porous LDH catalysts are in many cases designed by complexing with metal nanoparticles, oxides, and metal complexes. It should be emphasized that porosity is also advantageous for successful loading of these co-catalysts.

Recently, increasing attention has been devoted to electrocatalytic reactions, oxygen evolution reaction (OER), hydrogen evolution reaction (HER), overall water splitting (OWS) on LDH-based catalysts with unique porous structures (**Table.7**). For these applications, electrical conductivity of LDH-based electrodes is required to be increased and which in turn, the external power to be reduced. At the same time, active sites should be increased to boost the reaction. The complexation of porous LDH with conductive supports, such as metal and carbon-based materials (multiwalled carbon nanotube (CNT), carbon quantum dots (CQD), and graphene sheets), is a widely-employed strategy for this purpose. Electrochemically active metal elements such as Ni, Fe, Co, that can take various valence states, are selected to form LDHs.

Selective etching of hydroxide sheets to form micropores (defects) is another method for porous LDH and layered hydroxides for electro catalytic applications. (Huang et al., 2018; Liang et al., 2015; Xie et al., 2017) For example, Liang et al. et al reported synthesis of porous β-$Ni(OH)_2$

nanosheets from NiGa LDH nanoplates by applying an alkaline treatment through selective dissolution of amphoteric $Ga(OH)_3$. Since NiGa LDH and β-$Ni(OH)_2$ are layered materials with similar brucite-like crystal structures, topotactic conversion of NiGa LDH into β-$Ni(OH)_2$ occurs with preserving the overall morphology. As well as the direct use of hydroxide-based materials, they can be also employed as precursors for catalysts of metal sulfide, metals, MOF, and have been extensively investigated. A composite of metal hydroxides is known as a good precursor of homogeneous mixing of constitutive metal cations allowing for a targeted oxide phase with a stoichiometric composition by calcination at a relatively low temperature. For example, Takemoto et al. reported $ZnGa_2O_4$ catalysts prepared from a composite of metal hydroxides with a large hetero-interfaces of $Zn(OH)_2$ and $Ga(OH)_3$ nanoparticles. The material exhibits a stronger base strength even after the calcination at a high temperature, > 700 °C, compared to $ZnGa_2O_4$ prepared through a solid phase reaction.(Takemoto et al., 2020a) The enhanced surface is explained by the stoichiometric composition of the surface of $ZnGa_2O_4$. Such a catalytically-active surface of metal oxides can be more effectively used by coupling with mesoporosity by starting from mesoporous hydroxides. (Tarutani et al., 2016)

Table 6. Other catalytic applications of LDH taking advantage of unique porous structures.

Type	Reaction	Composition	complexed with	year	ref

Photocatalyst	CO_2 reduction	NiAl-	-	2018	(Tokudome et al., 2018)
	CO_2 reduction	CdAl-	Pd nanoparticles	2016	(Saliba et al., 2016)
	Photoelectrochemical water oxidation	NiFe-	WO_3 nanorod arrays	2016	(Fan et al., 2016)
	Cong red degradation	ZnAl-	$ZnCo_2O_4$	2016	(Yu et al., 2016b)
	Degradation of pesticides	MgAl-	decatungstate	2014	(Da Silva et al., 2014)
	O_2 generation	ZnCr-	titanate	2011	(Gunjakar et al., 2011)
Oxidation	Aerobic oxidation of alcohols	NiAl-	Ru/RuOx	2016	(Tan et al., 2016)
	Oxidation of Hydrocarbon	MgAl-	Iron(III) porphyrins	2009	(Halma et al., 2009)
	Dry reforming of methane	MgAl	Alumina	2022	(Taherian et al., 2022)
	Dry reforming of methane	NiMgAl	Alumina	2020	(Huang et al., 2020)
	Dry reforming of methane	NiMgAl	Alumina	2021	(Taherian et al., 2021)
Hydrogenation	Selective hydrogenation	MgAl-	Pd nanoparticles / porous alumina	2012	(Zhang et al., 2012)
Polymerization	Glycerol oligomerization	MgAl	-	2022	(Barros et al., 2022)

Table 7. Electrocatalytic applications of LDH taking advantage of unique porous structures. HER: Hydrogen Evolution Reaction; OER: Oxygen Evolution Reaction; OWS: Overall Water Splitting

Type	Reaction	Composition	complexed with	year	ref

Electrocatalyst	HER	NiV-	-	2020	(He et al., 2020)
	OWS	NiFe	Ni foam / Ag nanowire	2021	(Ma et al., 2021)
	OWS	CoCo	Cu foam / Cu_3P	2021	(Xu et al., 2021)
	OER	NiFe-	N-doped graphene quantum dots	2020	(Dong et al., 2020)
	OER	NiFe-	NiO / C	2020	(Li et al., 2020b)
	OER	NiFe-	Ni foam / ZnO	2020	(Luo et al., 2020)
	OER, ORR, OWS	NiFe-	Co_xMo_1P / Ni foam	2020	(Mai et al., 2020)
	OER	NiFe-	NiCoP / N-doped carbon / Ni foam	2020	(Nie et al., 2020)
	OER	NiFeW-	Ni foam	2020	(Wu et al., 2020a)
	OER	CoFe-	-	2020	(Zhao et al., 2020)
	ORR, OER	CoFe-	multiwalled carbon nanotube / reduced graphene oxide	2020	(Yang et al., 2020b)
	OER	CoNiAl-	ZIF-67 / Ni foam	2019	(Xu et al., 2019)
	OWS	NiFe-	Ni nanochain	2019	(Cai et al., 2019)
	OER	NiFe-	reduced graphene oxide / Ni foam	2019	(Gu et al., 2019)
	OER	NiVFe-	NiFe selenide	2019	(Song et al., 2019)
	OER	NiCoFe-	Cabon cloth	2018	(Cao et al., 2018b)
	OWS	NiFeV-	Ni foam	2018	(Dinh et al., 2018)
	OER	CoCo-	glassy carbon	2018	(Xu et al.,

				2018)
	OER	NiZn-	N-doped reduced graphene oxide	2017	(Nadeema et al., 2017)
	OER	CoFe-	Ni foam	2017	(Feng et al., 2017)
	OER	NiFe-	Porous graphitized carbon	2017	(Ni et al., 2017)
	OER	CoAl-	3D graphene	2016	(Ping et al., 2016)
	OER	NiFe-	Ni foam	2016	(Liu et al., 2015d)
	OER	NiFe-	reduced graphene oxide	2016	(Zhan et al., 2016)
	OER	NiFe-	reduced graphene oxide	2015	(Yu et al., 2015)
	Electrocatalytic oxidation of ethanol	MgFe-	-	2013	(Shao et al., 2013)

3.3 Energy storage & production

Catalytic and electrochemical characteristics of LDH have attracted many attention to generate and store energy through an environmentally benign process. Transesterification of triglycerides for biodiesel is one of the examples of the effective use of LDHs for production of green energy. LDH are safe, benign and effective solid base catalyst compared with conventional NaOH aqueous solution catalyst, which is harmful to the environment, human health, and production machines. A. F. Lee et al., reported that introduction of hierarchical meso/macroporous structure using sacrificial polystyrene sphere templates. (Woodford et al., 2012) Obtained porous LDH showed a fast methanol transesterification reaction because the meso/macropores improved the diffusion of viscous raw materials and increased accessible reaction sites (**Fig. 11**). Calcination

of LDHs is an effective strategy to achieve superior catalyst because calcination leads to increasing not only specific surface area but also the basicity of LDHs It is demonstrated that calcination of LDH increased specific surface area, from 85.32 to 223.52 m^2/g, and basic site densities, from 1.29 to 14.64 μmol/m^2, which improved functionality for biodiesel production. (Sun et al., 2019)

Electrochemically active LDH, composed of transition metal elements, are known as conventional battery materials, and their functionalities were improved by the introduction of macropores and mesopores.(Liu et al., 2015e; Meng et al., 2019; Shao et al., 2012; Song et al., 2012) These electrochemically active LDHs are employed as battery type electrodes of hybrid capacitors more recently. LDH show poor electron conductivity, therefore, compositing with conductive materials, such as transition metal oxides (Dai et al., 2019) and carbon-based materials (Zhu et al., 2020), or direct crystallization on conductive metal foams are a general approach to construct devices. **Table 8** summarizes the characteristics of porous LDH materials-based hybrid supercapacitor. It was reported that compositing with carbon-based materials increased not only conductivity but also specific surface area.(Zhao et al., 2014) The pecific surface area (198 m^2/g) and pore volume (0.38 cm^3/g) of NiMn-LDH/CNT were larger than the respective materials; 53 m^2/g and 0.12 cm^3/g for NiMn-LDH and 78 m^2/g and 0.16 cm^3/g for CNT. The formed textural pores worked as mesochannels and effectively transported liquid and ions, which resulted in high capacity, energy density, and power density of assembled hybrid capacitors. In the case of LDH-based materials with hollow structures, macrochannels were introduced in addition to mesochannels, which effectively transport liquid containing OH^- to improve the progress of electrochemical reactions. (Bai et al., 2017)

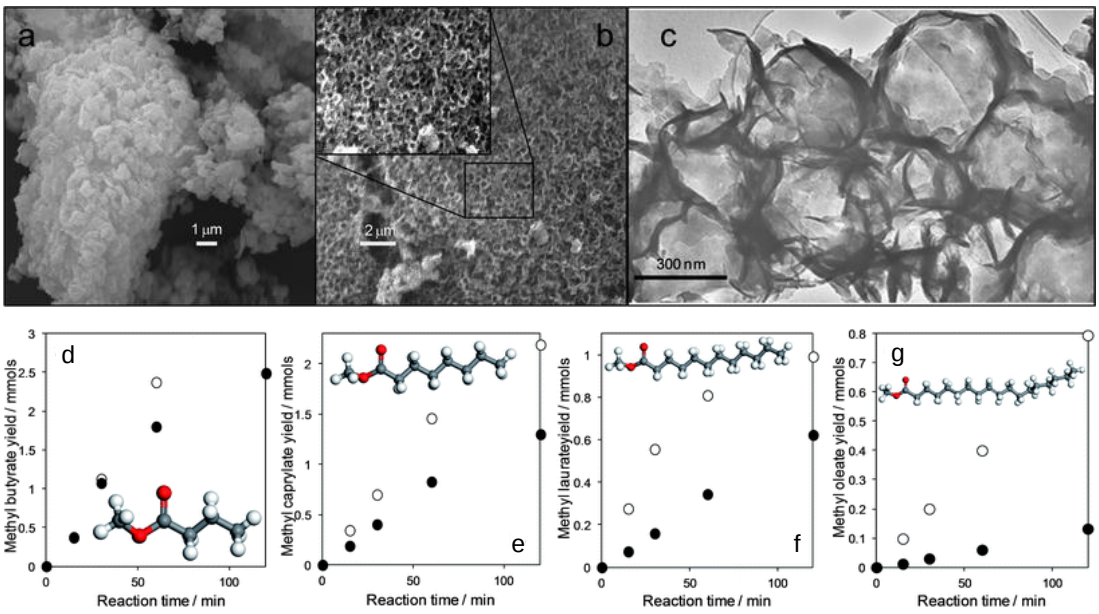

Fig. 11. SEM images of (a) conventional LDHs and (b) SEM and (c) TEM images of macroporous LDHs. Fatty acid methyl esters production via conventional LDHs (•) and macroporous LDHs (○) catalysed methanol transesterification of (d) tributyrin, (e) tricaprylin, (f) trilaurin and (g) triolein. Reproduced from Ref. (Woodford et al., 2012) with permission from RSC publishing.

Materials	Pore structure	Specific surface area / $m^2\ g^{-1}$	Potential window / V	Capacitance / $F\ g^{-1}$	Energy density / $Wh\ kg^{-1}$	Power density / $W\ kg^{-1}$	Ref
CoNi LDH/Co_3O_4//activated carbon	Textural pore	152	1.5	148.4	46.4−31.5	750.4−4500	(Dai et al., 2019)
CoNiZn LDH/graphene oxide //activated carbon	Textural pore	178	1.7	182.56	64.91−33.73	800−7999.21	(Zhu et al., 2020)
MnNi LDH/carbon nanotube //reduced graphene oxide/carbon nanotube	Textural pore	198	1.7	221	88.3−57.1	850−17200	(Zhao et al., 2014)
MXene-derived carbon/MnNi LDH //porous carbon nanosheets	Textural pore	190	1.6	56.4	45.2−20	802−12203	(Zhu et al., 2019)
CoAl LDH//activated carbon	Textural pore	332	1.5	125	44.8−35.5	850−27300	(Liu et al., 2016)
CoNi LDH/graphene//activated carbon	Hollow structure	219	1.7	170.9	68.0−23.96	594.9−4759.1	(Bai et al., 2017)
CoNi LDH//activated carbon	Hollow structure	72	1.5	158	49.3−29.89	750−7525.6	(Tahir et al., 2020)
CoNi LDH/CN_x@N-doped graphene // CN_x@N-doped graphene	Hollow structure	268	1.5	80.3	41.2−14.9	14.45−425	(Hao et al., 2017)
CoNi LDH//activated carbon	Hollow structure	-	1.7	110.2	44.3−24.1	425−4250	(Li et al., 2017)

Table 8. Characteristics of hybrid capacitors composed of porous LDH-based materials.

3.4 Bio-applications

The structural and morphological two-dimensionality of LDH combined with their ability to sequester, adsorb and self-assemble with anionic organic or biologic species such as drugs, antibacterial agents, genes and biomacromolecules, make them promising biocompatible host materials for various applications in biomedical sciences (Laipan et al., 2020; Mishra et al., 2018; Ray et al., 2018; Rives et al., 2014). Amongst others, we can cite drug delivery and controlled release systems, as antibacterial agents, biocatalysts, and biosensor development, (Taviot-Guého et al., 2018) tissue engineering scaffold and coating for implant applications (Tan et al., 2020). Various researchers have pointed out that nanostructured LDH, leading to hierarchical architecture with high porosity combining mesopores and macropores and enhanced surface properties, generally display considerably improved performance in bio applications. Moreover, the ability of LDH nanoparticles to be involved in porous nanocomposites also appeared as a great advantage to develop efficient LDH based biomaterials and further tune their biocompatibility and diffusion properties.

Porous LDH phases and porous LDH nanocomposites have proven to be highly efficient as nano-reservoirs for drugs such as diclofenac (Tammaro et al., 2009), ibuprofen (Barkhordari et al., 2014; Gunawan and Xu, 2009), flurbiprofen axetil (Yang et al., 2015), amoxicillin (Valarezo et al., 2013), naproxen (Figueiredo et al., 2020). Recently, many studies focused on porous electrospun fibers. For instance, Gao et al. (Gao et al., 2017) synthesized fibers by electrospinning based on poly(ε-caprolactone) mixed with LDH intercalated by the non-steroidal anti-inflammatory drugs ibuprofen

and ketoprofen. The authors showed that the nanocomposites fibers displayed slower sustained release of drugs compared to both pure drugs intercalated LDH and drug/ poly(ε-caprolactone) fibers (**Figs. 12 a and b**) with 44-48% and 20-25% of released for ibuprofen and ketoprofen respectively. Mats of electrospun fibers modified with drug loaded LDH were also investigated as bone tissue engineered scaffolds to promote cell adhesion and proliferation and then accelerate the tissue regeneration. (Belgheisi et al., 2020). Following a similar strategy an antimicrobial system based on electrospun poly(lactic acid) scaffold containing MgAl-LDH intercalated with silver sulfadiazine, an antibiotic being able to control bacterial infection was designed. Such porous nanocomposite scaffold gives place to a slow release of the active molecules displaying an interesting antimicrobial activity and a good biocompatibility of great interest for transdermal applications and antimicrobial wound dressings. (Malafatti et al., 2020)

LDH based hydrogels involving well-dispersed LDH and silver nanoparticles also exhibited interesting antimicrobial properties. (Boccalon et al., 2020; Cao et al., 2018a) For instance, a 3D interconnected macroporous scaffold with pore size in the range of 100-300 μm, obtained from a mixture of MgSrFe LDH and chitosan with well-dispersed Ag nanoparticles on its surface exhibited excellent cytocompatibility, osteoinductivity and antibacterial properties (**Fig. 12 c**). It was also evidenced that LDH chitosan scaffolds having three-dimensional interconnected macroporous network act efficiently as therapeutic bone scaffolds, enhancing stem cell osteogenic differentiation and bone regeneration. The loading of the scaffolds with pilithrin-α enhanced their ability for cell differentiation (**Fig. 12 d**).(Chen et al., 2017)

Lee and coll. (Lee et al., 2017) also reported on a 2D/3D nanocomposite system promising as an injectable stem cell system. The presence of 2D LDH particles

enhanced the mechanical properties of the (poly(ethylene glycol)-poly(L-alanine)-poly(L-aspartate) thermogel especially the rigidity, slowed down the release of kartogenin a soluble factor of mesenchymal stem cells differentiation and improved the interaction between the cell and the material.

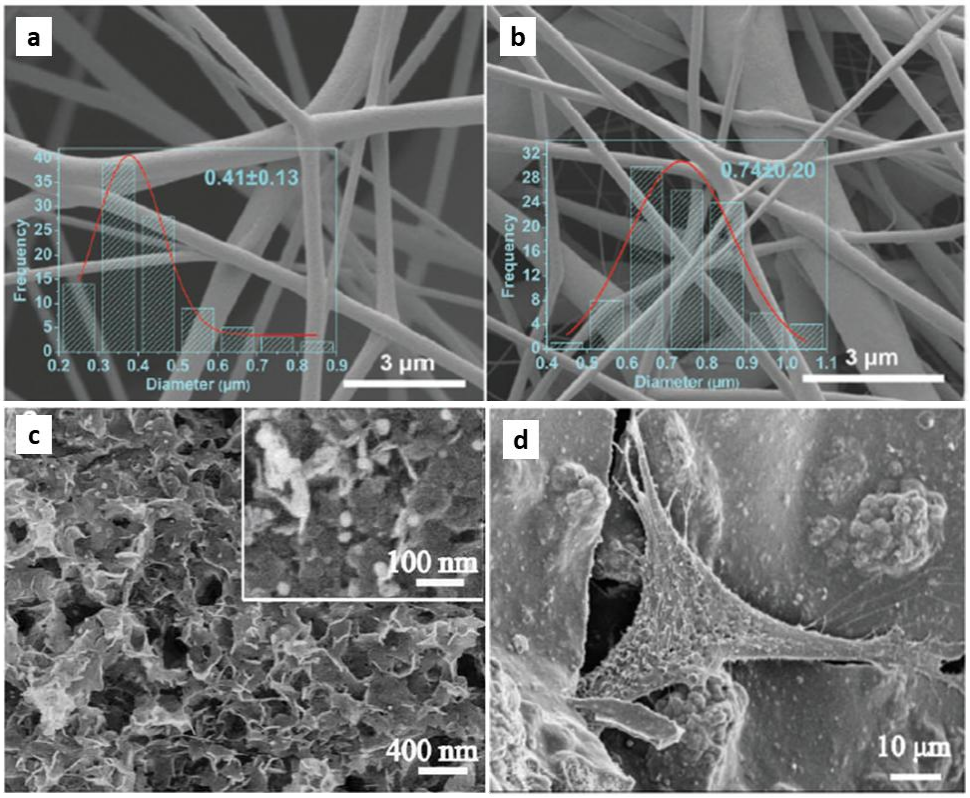

Fig. 12. SEM images of poly(ε-caprolactone) fibers containing a) 5% ibuprofen intercalated LDH, b) 5% ketoprofen intercalated LDH, c) Ag MgSrFe LDH / chitosan composite scaffold and d) bone cells on pilithrin-α loaded MgAl LDH chitosan scaffold (40 μM). Adapted from (Gao et al., 2017) and (Chen et al., 2017). Copyright (2017), with permission from the Royal Society Elsevier. Reprinted from (Cao et al., 2018a) , Copyright (2017), with permission from John Wiley and Sons.

4. Conclusion

Processing porous architectures based on LDHs has been overviewed. Various techniques of soft- and hard-templating, post-treatments, compositing with supports/other functional materials, have been developed to tune and enhance the physical and chemical characteristics of LDHs. Simultaneous control of the crystallization, nano-and macro structuration is required to achieve desirable porous structures, and for this end, processes are designed to properly control reactions such as, dissolution-(re)crystallization, heterogeneous nucleation, interaction with organic molecules/polymers, and solvation/hydration. In contrast passive inorganic supports materials accommodating functional centers, the original features of LDH crystals can be enhanced by introducing unique porosity thanks to increased surface area and better molecular/ion diffusion. As a result, the introduced porosity indeed has displayed considerable advantages for various applications such as adsorption for environmental purposes, energy production, storage and conversion, photo-and electro-catalysis, and biosciences. The soft chemical features of LDHs on their synthesis and applications, and the capability of using ubiquitous metal elements will further pave a way to develop functional materials in an environmental-friendly way, where the processing of 3D porous architectures summarized in this chapter is ready to be integrated.

Declaration of Competing Interest

The authors declare that they have no known competing financial interests or personal relationships that could have appeared to influence the work reviews in this paper.

References

Abolghasemi, M.M., Yousefi, V., 2014. Three dimensionally honeycomb layered double hydroxides framework as a novel fiber coating for headspace solid-phase microextraction of phenolic compounds. J Chromatogr A 1345, 9-16.

Abushrenta, N., Wu, X., Wang, J., Liu, J., Sun, X., 2015. Hierarchical Co-based Porous Layered Double Hydroxide Arrays Derived via Alkali Etching for High-performance Supercapacitors. Scientific Reports 5.

Badar, M., Rahim, M.I., Kieke, M., Ebel, T., Rohde, M., Hauser, H., Behrens, P., Mueller, P.P., 2015. Controlled drug release from antibiotic-loaded layered double hydroxide coatings on porous titanium implants in a mouse model. Journal of Biomedical Materials Research Part A 103, 2141-2149.

Bai, X., Liu, Q., Lu, Z., Liu, J., Chen, R., Li, R., Song, D., Jing, X., Liu, P., Wang, J., 2017. Rational Design of Sandwiched Ni–Co Layered Double Hydroxides Hollow Nanocages/Graphene Derived from Metal–Organic Framework for Sustainable Energy Storage. ACS Sustainable Chemistry & Engineering 5, 9923-9934.

Barkhordari, S., Yadollahi, M., Namazi, H., 2014. pH sensitive nanocomposite hydrogel beads based on carboxymethyl cellulose/layered double hydroxide as drug delivery systems. Journal of Polymer Research 21, 454.

Barros, F.J.S., Liu, Y., Paula, C.D., de Luna, F.M.T., Rodriguez-Castellon, E., Silveira Vieira, R., 2022. Enhancement of the catalytic activity of Mg/Al layered double hydroxide for glycerol oligomers production. Dalton Trans 51, 3213-3224.

Basile, F., Benito, P., Del Gallo, P., Fornasari, G., Gary, D., Rosetti, V., Scavetta, E., Tonelli, D., Vaccari, A., 2008. Highly conductive Ni steam reforming catalysts prepared by electrodeposition. Chemical Communications, 2917-2919.

Basile, F., Benito, P., Fornasari, G., Rosetti, V., Scavetta, E., Tonelli, D., Vaccari, A., 2009. Electrochemical synthesis of novel structured catalysts for H2 production. Applied Catalysis B: Environmental 91, 563-572.

Belgheisi, G., Nazarpak, M.H., Hashjin, M.S., 2020. Bone tissue engineering electrospun scaffolds based on layered double hydroxides with the ability to release vitamin D3: Fabrication, characterization and in vitro study. Applied Clay Science 185, 105434.

Benito, P., de Nolf, W., Nuyts, G., Monti, M., Fornasari, G., Basile, F., Janssens, K., Ospitali, F., Scavetta, E., Tonelli, D., Vaccari, A., 2014. Role of Coating-Metallic Support Interaction in the Properties of Electrosynthesized Rh-Based Structured Catalysts. ACS Catalysis 4, 3779-3790.

Boccalon, E., Pica, M., Romani, A., Casciola, M., Sterflinger, K., Pietrella, D., Nocchetti, M., 2020. Facile preparation of organic-inorganic hydrogels containing silver or essential oil with antimicrobial effects. Applied Clay Science 190, 105567.

Brezesinski, T., Wang, J., Tolbert, S.H., Dunn, B., 2010. Ordered mesoporous α-MoO_3 with iso-oriented nanocrystalline walls for thin-film pseudocapacitors. Nature Materials 9, 146-151.

Cai, Z., Bu, X., Wang, P., Su, W., Wei, R., Ho, J.C., Yang, J., Wang, X., 2019. Simple and cost effective fabrication of 3D porous core-shell Ni nanochains@NiFe layered double hydroxide nanosheet bifunctional electrocatalysts for overall water splitting. Journal of Materials Chemistry A 7, 21722-21729.

Cao, D., Xu, Z., Chen, Y., Ke, Q., Zhang, C., Guo, Y., 2018a. Ag-loaded MgSrFe-layered double hydroxide/chitosan composite scaffold with enhanced osteogenic and antibacterial property for bone engineering tissue. Journal of Biomedical Materials Research Part B: Applied Biomaterials 106, 863-873.

Cao, J., Li, J., Li, L., Zhang, Y., Cai, D., Chen, D., Han, W., 2019. Mn-Doped Ni/Co LDH Nanosheets Grown on the Natural N-Dispersed PANI-Derived Porous Carbon Template for a Flexible Asymmetric Supercapacitor. ACS Sustainable Chemistry & Engineering 7, 10699-10707.

Cao, L.M., Wang, J.W., Zhong, D.C., Lu, T.B., 2018b. Template-directed synthesis of sulphur doped NiCoFe layered double hydroxide porous nanosheets with enhanced electrocatalytic activity for the oxygen evolution reaction. Journal of Materials Chemistry A 6, 3224-3230.

Cao, W., Muhammad, F., Cheng, Y., Zhou, M., Wang, Q., Lou, Z., Li, Z., Wei, H., 2018c. Acid Susceptible Ultrathin Mesoporous Silica Coated on Layered Double Hydroxide Nanoplates for pH Responsive Cancer Therapy. ACS Applied Bio Materials 1, 928-935.

Carja, G., Nakamura, R., Aida, T., Niiyama, H., 2001. Textural properties of layered double hydroxides: Effect of magnesium substitution by copper or iron. Microporous and Mesoporous Materials 47, 275-284.

Chane-Ching, J.Y., Cobo, F., Aubert, D., Harvey, H.G., Airiau, M., Corma, A., 2005. A general method for the synthesis of nanostructured large-surface-area materials through the self-assembly of functionalized nanoparticles. Chemistry - A European Journal 11, 979-987.

Chen, C., Byles, C.F.H., Buffet, J.-C., Rees, N.H., Wu, Y., O'Hare, D., 2016. Core–shell zeolite@aqueous miscible organic-layered double hydroxides. Chemical Science 7, 1457-1461.

Chen, C., Wangriya, A., Buffet, J.C., O'Hare, D., 2015. Tuneable ultra high specific surface area Mg/Al-CO3 layered double hydroxides. Dalton Transactions 44, 16392-16398.

Chen, H., Hu, L., Chen, M., Yan, Y., Wu, L., 2014. Nickel–Cobalt Layered Double Hydroxide Nanosheets for High-performance Supercapacitor Electrode Materials. Advanced Functional Materials 24, 934-942.

Chen, L., Wang, J., Shen, X., Li, X., Duan, C., 2019. ZIF-67@Co-LDH yolk–shell spheres with micro-/meso-porous structures as vehicles for drug delivery. Inorganic Chemistry Frontiers 6, 3140-3145.

Chen, S., Zhao, L., Wei, W., Li, Y., Mi, L., 2020. A novel strategy to synthesize NiCo layered double hydroxide nanotube from metal organic framework composite for high-performance supercapacitor. Journal of Alloys and Compounds 831, 154794.

Chen, Y.-X., Zhu, R., Ke, Q.-F., Gao, Y.-S., Zhang, C.-Q., Guo, Y.-P., 2017. MgAl layered double hydroxide/chitosan porous scaffolds loaded with PFTα to promote bone regeneration. Nanoscale 9, 6765-6776.

Choudary, B.M., Jaya, V.S., Reddy, B.R., Kantam, M.L., Rao, M.M., Madhavendra, S.S., 2005. Synthesis, characterization, ion exchange, and catalytic properties of nanobinary and ternary metal oxy/hydroxides. Chemistry of Materials 17, 2740-2743.

Costantino, U., Marmottini, F., Nocchetti, M., Vivani, R., 1998. New synthetic routes to hydrotalcite-like compounds - Characterisation and properties of the obtained materials. European Journal of Inorganic Chemistry, 1439-1446.

Creasey, J.J., Parlett, C.M.A., Manayil, J.C., Isaacs, M.A., Wilson, K., Lee, A.F., 2015. Facile route to conformal hydrotalcite coatings over complex architectures: a hierarchically ordered nanoporous base catalyst for FAME production. Green Chemistry 17, 2398-2405.

Crossland, E.J.W., Noel, N., Sivaram, V., Leijtens, T., Alexander-Webber, J.A., Snaith, H.J., 2013. Mesoporous TiO 2 single crystals delivering enhanced mobility and optoelectronic device performance. Nature 495, 215-219.

Da Silva, E.S., Prevot, V., Forano, C., Wong-Wah-Chung, P., Burrows, H.D., Sarakha, M., 2014. Heterogeneous photocatalytic degradation of pesticides using decatungstate intercalated macroporous layered double hydroxides. Environmental Science and Pollution Research 21, 11218-11227.

Dai, X., Dai, Y., Lu, J., Pu, L., Wang, W., Jin, J., Ma, F., Tie, N., 2019. Cobalt oxide nanocomposites modified by NiCo-layered double hydroxide nanosheets as advanced electrodes for supercapacitors. Ionics 26, 2501-2511.

Daud, M., Hai, A., Banat, F., Wazir, M.B., Habib, M., Bharath, G., Al-Harthi, M.A., 2019. A review on the recent advances, challenges and future aspect of layered double hydroxides (LDH) – Containing hybrids as promising adsorbents for dyes removal. Journal of Molecular Liquids 288.

Decher, G., 1997. Fuzzy Nanoassemblies: Toward Layered Polymeric Multicomposites. Science 277, 1232.

Dinh, K.N., Zheng, P., Dai, Z., Zhang, Y., Dangol, R., Zheng, Y., Li, B., Zong, Y., Yan, Q., 2018. Ultrathin Porous NiFeV Ternary Layer Hydroxide Nanosheets as a Highly Efficient Bifunctional Electrocatalyst for Overall Water Splitting. Small 14.

Dong, Q., Shuai, C., Mo, Z., Liu, Z., Liu, G., Wang, J., Chen, Y., Liu, W., Liu, N., Guo, R., 2020. Nitrogen-doped graphene quantum dots anchored on NiFe layered double-hydroxide nanosheets catalyze the oxygen evolution reaction. New Journal of Chemistry 44, 17744-17752.

Dreyer, D.R., Murali, S., Zhu, Y., Ruoff, R.S., Bielawski, C.W., 2011. Reduction of graphite oxide using alcohols. Journal of Materials Chemistry 21, 3443-3447.

Duan, X., Evans, D.G., 2006. Layered Double Hydroxides.

El Hassani, K., Jabkhiro, H., Kalnina, D., Beakou, B.H., Anouar, A., 2019. Effect of drying step on layered double hydroxides properties: Application in reactive dye intercalation. Applied Clay Science 182.

Fan, X., Gao, B., Wang, T., Huang, X., Gong, H., Xue, H., Guo, H., Song, L., Xia, W., He, J., 2016.

Layered double hydroxide modified WO_3 nanorod arrays for enhanced photoelectrochemical water splitting. Applied Catalysis A: General 528, 52-58.

Fang, D., Huang, L., Fan, J., Xiao, H., Wu, G., Wang, Y., Zeng, Z., Shen, F., Deng, S., Ji, F., 2022. New insights into the arrangement pattern of layered double hydroxide nanosheets and their ion-exchange behavior with phosphate. Chemical Engineering Journal 441.

Faour, A., Mousty, C., Prevot, V., Devouard, B., De Roy, A., Bordet, P., Elkaim, E., Taviot-Gueho, C., 2012. Correlation among structure, microstructure, and electrochemical properties of NiAl-CO_3 layered double hydroxide thin films. Journal of Physical Chemistry C 116, 15646-15659.

Feng, L., Li, A., Li, Y., Liu, J., Wang, L., Huang, L., Wang, Y., Ge, X., 2017. A Highly Active CoFe Layered Double Hydroxide for Water Splitting. ChemPlusChem 82, 483-488.

Figueiredo, M.P., Layrac, G., Hébraud, A., Limousy, L., Brendle, J., Schlatter, G., Constantino, V.R.L., 2020. Design of 3D multi-layered electrospun membranes embedding iron-based layered double hydroxide for drug storage and control of sustained release. European Polymer Journal 131, 109675.

Forano, C., Costantino, U., Prévot, V., Gueho, C.T., 2013. Layered double hydroxides (LDH), Developments in Clay Science, pp. 745-782.

Gao, Y., Teoh, T.W., Wang, Q., Williams, G.R., 2017. Electrospun organic–inorganic nanohybrids as sustained release drug delivery systems. Journal of Materials Chemistry B 5, 9165-9174.

Gash, A.E., Tillotson, T.M., Satcher Jr, J.H., Poco, J.F., Hrubesh, L.W., Simpson, R.L., 2001. Use of epoxides in the sol-gel synthesis of porous iron(III) oxide monoliths from Fe(III) salts. Chemistry of Materials 13, 999-1007.

Géraud, E., Prévot, V., Ghanbaja, J., Leroux, F., 2006. Macroscopically Ordered Hydrotalcite-Type Materials Using Self-Assembled Colloidal Crystal Template. Chemistry of Materials 18, 238-240.

Géraud, E., Rafqah, S., Sarakha, M., Forano, C., Prevot, V., Leroux, F., 2008. Three Dimensionally Ordered Macroporous Layered Double Hydroxides: Preparation by Templated Impregnation/Coprecipitation and Pattern Stability upon Calcination. Chemistry of Materials 20, 1116-1125.

Ghani, M., Frizzarin, R.M., Maya, F., Cerdà, V., 2016. In-syringe extraction using dissolvable layered double hydroxide-polymer sponges templated from hierarchically porous coordination polymers. Journal of Chromatography A 1453, 1-9.

Goh, K.H., Lim, T.T., Dong, Z., 2008. Application of layered double hydroxides for removal of oxyanions: a review. Water Res 42, 1343-1368.

Gómez-Avilés, A., Aranda, P., Ruiz-Hitzky, E., 2016. Layered double hydroxide/sepiolite heterostructured materials. Applied Clay Science 130, 83-92.

Gu, Y., Wang, Y., An, W., Men, Y., Rui, Y., Fan, X., Li, B., 2019. A novel strategy to boost the oxygen evolution reaction activity of NiFe-LDHs with in situ synthesized 3D porous reduced graphene oxide matrix as both the substrate and electronic carrier. New Journal of Chemistry 43, 6555-6562.

Gu, Z., Atherton, J.J., Xu, Z.P., 2015. Hierarchical layered double hydroxide nanocomposites: Structure, synthesis and applications. Chemical Communications 51, 3024-3036.

Gunawan, P., Xu, R., 2008. Synthesis of unusual coral-like layered double hydroxide microspheres in a nonaqueous polar solvent/surfactant system. Journal of Materials Chemistry 18, 2112-2120.

Gunawan, P., Xu, R., 2009. Direct Assembly of Anisotropic Layered Double Hydroxide (LDH) Nanocrystals on Spherical Template for Fabrication of Drug-LDH Hollow Nanospheres. Chemistry of Materials 21, 781-783.

Gunjakar, J.L., Kim, T.W., Kim, H.N., Kim, I.Y., Hwang, S.J., 2011. Mesoporous layer-by-layer ordered nanohybrids of layered double hydroxide and layered metal oxide: Highly active visible light photocatalysts with improved chemical stability. Journal of the American Chemical Society 133, 14998-15007.

Guoxiang, P., Xinhui, X., Jingshan, L., Feng, C., Zhihong, Y., Hongjin, F., 2014. Preparation of CoAl layered double hydroxide nanoflake arrays and their high supercapacitance performance. Applied Clay Science 102, 28-32.

Gwak, G.-H., Kwon, N.K., Lee, W.-J., Paek, S.-M., Kim, S.Y., Oh, J.-M., 2017. Controlled Crystal Growth of Two-Dimensional Layered Nanomaterials in Hydrogel via a Modified Electrical Double Migration Method. Crystal Growth & Design 17, 6596-6602.

Hai, B., Zou, Y., 2015. Carbon cloth supported NiAl-layered double hydroxides for flexible application and highly sensitive electrochemical sensors. Sensors and Actuators B: Chemical 208, 143-150.

Halma, M., Castro, K.A.D.d.F., Prévot, V., Forano, C., Wypych, F., Nakagaki, S., 2009. Immobilization of anionic iron(III) porphyrins into ordered macroporous layered double hydroxides and investigation of catalytic activity in oxidation reactions. Journal of Molecular Catalysis A: Chemical 310, 42-50.

Han, B., Cheng, G., Zhang, E., Zhang, L., Wang, X., 2018. Three dimensional hierarchically porous ZIF-8 derived carbon/LDH core-shell composite for high performance supercapacitors. Electrochimica Acta 263, 391-399.

Hao, X., Jiang, Z., Tian, X., Hao, X., Jiang, Z.-J., 2017. Facile Assembly of Co-Ni Layered Double Hydroxide Nanoflakes on Carbon Nitride Coated N-doped Graphene Hollow Spheres with High Electrochemical Capacitive Performance. Electrochimica Acta 253, 21-30.

He, D., Cao, L., Huang, J., Kajiyoshi, K., Wu, J., Wang, C., Liu, Q., Yang, D., Feng, L., 2020. In-situ optimizing the valence configuration of vanadium sites in NiV-LDH nanosheet arrays for enhanced hydrogen evolution reaction. Journal of Energy Chemistry 47, 263-271.

Hibino, T., 2020. Deterioration of anion-adsorption abilities of layered double hydroxides synthesized in agarose gel. Applied Clay Science 186, 105435.

Hu, H., Liu, J., Xu, Z., Zhang, L., Cheng, B., Ho, W., 2019. Hierarchical porous Ni/Co-LDH hollow dodecahedron with excellent adsorption property for Congo red and Cr(VI) ions. Applied Surface Science 478, 981-990.

Hu, Z., Chen, G., 2014. Novel nanocomposite hydrogels consisting of layered double hydroxide with ultrahigh tensibility and hierarchical porous structure at low inorganic content. Advanced Materials 26, 5950-5956.

Huang, H., Xu, J., Wei, K., Xu, Y.J., Choi, C.K.K., Zhu, M., Bian, L., 2016. Bioactive Nanocomposite Poly (Ethylene Glycol) Hydrogels Crosslinked by Multifunctional Layered Double Hydroxides Nanocrosslinkers. Macromolecular Bioscience 16, 1019-1026.

Huang, J., Yan, Y., Saqline, S., Liu, W., Liu, B., 2020. High performance Ni catalysts prepared by freeze drying for efficient dry reforming of methane. Applied Catalysis B: Environmental 275.

Huang, L., Chen, R., Xie, C., Chen, C., Wang, Y., Zeng, Y., Chen, D., Wang, S., 2018. Rapid cationic defect and anion dual-regulated layered double hydroxides for efficient water oxidation. Nanoscale 10, 13638-13644.

Huang, P., Liu, J., Wei, F., Zhu, Y., Wang, X., Cao, C., Song, W., 2017. Size-selective adsorption of anionic dyes induced by the layer space in layered double hydroxide hollow microspheres. Materials Chemistry Frontiers 1, 1550-1555.

Huang, W., Yu, X., Li, D., 2015. Adsorption removal of Congo red over flower-like porous microspheres derived from Ni/Al layered double hydroxide. RSC Advances 5, 84937-84946.

Inagaki, S., Guan, S., Ohsuna, T., Terasaki, O., 2002. An ordered mesoporous organosilica hybrid material with a crystal-like wall structure. Nature 416, 304-307.

Intasa-Ard, S., Bureekaew, S., Ogawa, M., 2019. Efficient production of MgAl layered double hydroxide nanoparticle. Journal of the Ceramic Society of Japan 127, 11-17.

Ji, C., Wang, Y., Zhao, N., 2019. Synthesis of CuAl hydrotalcite-SBA-15 composites and CO_2 capture using the sorbent. Applied Surface Science 481, 337-343.

Jia, D., Gao, H., Zhao, J., Xing, L., Chen, X., Huang, X., Dang, R., Wang, G., 2020. Self-templating synthesis of hollow NiFe hydroxide nanospheres for efficient oxygen evolution reaction. Electrochimica Acta 357.

Jia, G., Hu, Y., Qian, Q., Yao, Y., Zhang, S., Li, Z., Zou, Z., 2016. Formation of Hierarchical Structure Composed of (Co/Ni)Mn-LDH Nanosheets on MWCNT Backbones for Efficient Electrocatalytic Water Oxidation. ACS Applied Materials & Interfaces 8, 14527-14534.

Jia, Y.-H., Liu, Z.-H., 2019. Preparation of borate anions intercalated MgAl-LDHs microsphere and its calcinated product with superior adsorption performance for Congo red. Colloids and Surfaces A: Physicochemical and Engineering Aspects 575, 373-381.

Jiang, S.-D., Bai, Z.-M., Tang, G., Song, L., Stec, A.A., Hull, T.R., Hu, Y., Hu, W.-Z., 2014. Synthesis of Mesoporous Silica@Co–Al Layered Double Hydroxide Spheres: Layer-by-Layer Method and Their Effects on the Flame Retardancy of Epoxy Resins. ACS Applied Materials & Interfaces 6, 14076-14086.

Jiang, Z., Li, Z., Qin, Z., Sun, H., Jiao, X., Chen, D., 2013. LDH nanocages synthesized with MOF templates and their high performance as supercapacitors. Nanoscale 5, 11770-11775.

Julklang, W., Wangriya, A., Golman, B., 2017. Fabrication of layered double hydroxide microspheres by spray drying of nanoparticles: Effects of process conditions. Materials Letters 209, 429-432.

Karthik Kiran, S., Shukla, S., Struck, A., Saxena, S., 2019. Surface Engineering of Graphene Oxide Shells Using Lamellar LDH Nanostructures. ACS Applied Materials and Interfaces 11, 20232-20240.

Katagiri, K., Shishijima, Y., Koumoto, K., Inumaru, K., 2018. Preparation of pH-Responsive Hollow Capsules via Layer-by-Layer Assembly of Exfoliated Layered Double Hydroxide Nanosheets and Polyelectrolytes. J Nanosci Nanotechnol 18, 110-115.

Kim, B.-K., Gwak, G.-H., Okada, T., Oh, J.-M., 2018. Effect of particle size and local disorder on specific surface area of layered double hydroxides upon calcination-reconstruction. Journal of Solid State Chemistry 263, 60-64.

Kim, T.W., Sahimi, M., Tsotsis, T.T., 2008. Preparation of Hydrotalcite Thin Films Using an Electrophoretic Technique. Industrial & Engineering Chemistry Research 47, 9127-9132.

Kresge, C.T., Leonowicz, M.E., Roth, W.J., Vartuli, J.C., Beck, J.S., 1992. Ordered mesoporous molecular sieves synthesized by a liquid-crystal template mechanism. Nature 359, 710-712.

Lai, F., Huang, Y., Miao, Y.E., Liu, T., 2015. Controllable preparation of multi-dimensional hybrid materials of nickel-cobalt layered double hydroxide nanorods/nanosheets on electrospun carbon nanofibers for high-performance supercapacitors. Electrochimica Acta 174, 456-463.

Laipan, M., Yu, J., Zhu, R., Zhu, J., Smith, A.T., He, H., O'Hare, D., Sun, L., 2020. Functionalized layered double hydroxides for innovative applications. Materials Horizons 7, 715-745.

Lee, G., Na, W., Kim, J., Lee, S., Jang, J., 2019. Improved electrochemical performances of MOF-derived Ni–Co layered double hydroxide complexes using distinctive hollow-in-hollow structures. Journal of Materials Chemistry A 7, 17637-17647.

Lee, S.S., Choi, G.E., Lee, H.J., Kim, Y., Choy, J.-H., Jeong, B., 2017. Layered Double Hydroxide and Polypeptide Thermogel Nanocomposite System for Chondrogenic Differentiation of Stem Cells. ACS Applied Materials & Interfaces 9, 42668-42675.

Lei, C., Pi, M., Kuang, P., Guo, Y., Zhang, F., 2017. Organic dye removal from aqueous solutions by hierarchical calcined Ni-Fe layered double hydroxide: Isotherm, kinetic and mechanism studies. J Colloid Interface Sci 496, 158-166.

Leroux, F., Adachi-Pagano, M., Intissar, M., Chauvière, S., Forano, C., Besse, J.-P., 2001. Delamination and restacking of layered double hydroxides. Journal of Materials Chemistry 11, 105-112.

Li, F., Jiang, X., Evans, D.G., Duan, X., 2005. Structure and Basicity of Mesoporous Materials from Mg/Al/In Layered Double Hydroxides Prepared by Separate Nucleation and Aging Steps Method. Journal of Porous Materials 12, 55-63.

Li, L., Ma, R., Iyi, N., Ebina, Y., Takada, K., Sasaki, T., 2006. Hollow nanoshell of layered double hydroxide. Chemical Communications, 3125-3127.

Li, L., Shi, J., 2008. In situ assembly of layered double hydroxide nano-crystallites within silica

mesopores and its high solid base catalytic activity. Chemical Communications, 996-998.
Li, M., Yuan, P., Guo, S., Liu, F., Cheng, J.P., 2017. Design and synthesis of Ni-Co and Ni-Mn layered double hydroxides hollow microspheres for supercapacitor. International Journal of Hydrogen Energy 42, 28797-28806.
Li, N., Chang, Z., Dang, H., Zhan, Y., Lou, J., Wang, S., Attique, S., Li, W., Zhou, H., Sun, C., 2020a. Deep eutectic solvents assisted synthesis of MgAl layered double hydroxide with enhanced adsorption toward anionic dyes. Colloids and Surfaces A: Physicochemical and Engineering Aspects 591.
Li, S., Mo, S., Li, J., Liu, H., Chen, Y., 2016. Promoted VOC oxidation over homogeneous porous CoXNiAlO composite oxides derived from hydrotalcites: Effect of preparation method and doping. RSC Advances 6, 56874-56884.
Li, X., Fan, M., Wei, D., Wang, X., Wang, Y., 2020b. Core-Shell NiO/C@NiFe-LDH Nanocomposite as an Efficient Electrocatalyst for Oxygen Evolution Reaction. Journal of the Electrochemical Society 167.
Li, Z., Shao, M., An, H., Wang, Z., Xu, S., Wei, M., Evans, D.G., Duan, X., 2015. Fast electrosynthesis of Fe-containing layered double hydroxide arrays toward highly efficient electrocatalytic oxidation reactions. Chemical Science 6, 6624-6631.
Li, Z., Yang, B., Zhang, S., Wang, B., Xue, B., 2014. A novel approach to hierarchical sphere-like ZnAl-layered double hydroxides and their enhanced adsorption capability. Journal of Materials Chemistry A 2, 10202-10210.
Liang, H., Li, L., Meng, F., Dang, L., Zhuo, J., Forticaux, A., Wang, Z., Jin, S., 2015. Porous Two-Dimensional Nanosheets Converted from Layered Double Hydroxides and Their Applications in Electrocatalytic Water Splitting. Chemistry of Materials 27, 5702-5711.
Liao, F., Yang, G., Cheng, Q., Mao, L., Zhao, X., Chen, L., 2022. Rational design and facile synthesis of Ni-Co-Fe ternary LDH porous sheets for high-performance aqueous asymmetric supercapacitor. Electrochimica Acta 428.
Lin, Y., Ruiyi, L., Zaijun, L., Junkang, L., Yinjun, F., Guangli, W., Zhiguo, G., 2013. Three-dimensional activated reduced graphene oxide nanocup/nickel aluminum layered double hydroxides composite with super high electrochemical and capacitance performances. Electrochimica Acta 95, 146-154.
Liu, C., Zhang, M., Pan, G., Lundehøj, L., Nielsen, U.G., Shi, Y., Hansen, H.C.B., 2019. Phosphate capture by ultrathin MgAl layered double hydroxide nanoparticles. Applied Clay Science 177, 82-90.
Liu, G., Wang, G., Guo, X., Hao, X., Jin, Z., 2022. Toilless sulfuration route to enhance the supercapacitor performance of nanoflower-like NiAl-layered double hydroxide. Journal of Electroanalytical Chemistry 916.
Liu, L., Wang, W., Hu, Y., 2015a. Layered double hydroxide-decorated flexible polyurethane foam: significantly improved toxic effluent elimination. RSC Advances 5, 97458-97466.
Liu, M., He, S., Miao, Y.E., Huang, Y., Lu, H., Zhang, L., Liu, T., 2015b. Eco-friendly synthesis of hierarchical ginkgo-derived carbon nanoparticles/NiAl-layered double hydroxide hybrid electrodes

toward high-performance supercapacitors. RSC Advances 5, 55109-55118.
Liu, X., Tian, W., Kong, X., Jiang, M., Sun, X., Lei, X., 2015c. Selective removal of thiosulfate from thiocyanate-containing water by a three-dimensional structured adsorbent: a calcined NiAl-layered double hydroxide film. RSC Advances 5, 87948-87955.
Liu, X., Wang, X., Yuan, X., Dong, W., Huang, F., 2015d. Rational composition and structural design of in situ grown nickel-based electrocatalysts for efficient water electrolysis. Journal of Materials Chemistry A 4, 167-172.
Liu, X., Zhou, A., Pan, T., Dou, Y., Shao, M., Han, J., Wei, M., 2016. Ultrahigh-rate-capability of a layered double hydroxide supercapacitor based on a self-generated electrolyte reservoir. Journal of Materials Chemistry A 4, 8421-8427.
Liu, Y., Fu, N., Zhang, G., Xu, M., Lu, W., Zhou, L., Huang, H., 2017. Design of Hierarchical Ni□Co@Ni□Co Layered Double Hydroxide Core–Shell Structured Nanotube Array for High-Performance Flexible All-Solid-State Battery-Type Supercapacitors. Advanced Functional Materials 27, 1605307.
Liu, Y., Wang, N., Diestel, L., Steinbach, F., Caro, J., 2014a. MOF membrane synthesis in the confined space of a vertically aligned LDH network. Chemical Communications 50, 4225-4227.
Liu, Y., Wang, N., Pan, J.H., Steinbach, F., Caro, J., 2014b. In Situ Synthesis of MOF Membranes on ZnAl-CO3 LDH Buffer Layer-Modified Substrates. Journal of the American Chemical Society 136, 14353-14356.
Liu, Y., Yang, Z., Xie, X., Huang, J., Wen, X., 2015e. Layered Double Oxides Nano-flakes Derived From Layered Double Hydroxides: Preparation, Properties and Application in Zinc/Nickel Secondary Batteries. Electrochimica Acta 185, 190-197.
Lu, X., Zhao, C., 2015. Electrodeposition of hierarchically structured three-dimensional nickel–iron electrodes for efficient oxygen evolution at high current densities. Nature Communications 6, 6616.
Luo, Y., Wu, Y., Wu, D., Huang, C., Xiao, D., Chen, H., Zheng, S., Chu, P.K., 2020. NiFe-Layered Double Hydroxide Synchronously Activated by Heterojunctions and Vacancies for the Oxygen Evolution Reaction. ACS Applied Materials and Interfaces 12, 42850-42858.
Lv, W., Mei, Q., Xiao, J., Du, M., Zheng, Q., 2017. 3D Multiscale Superhydrophilic Sponges with Delicately Designed Pore Size for Ultrafast Oil/Water Separation. Advanced Functional Materials 27, 1704293.
Lyu, H., Hu, K., Fan, J., Ling, Y., Xie, Z., Li, J., 2020. 3D hierarchical layered double hydroxide/carbon spheres composite with hollow structure for high adsorption of dye. Applied Surface Science 500.
Ma, K., Cheng, J.P., Liu, F., Zhang, X., 2016. Co-Fe layered double hydroxides nanosheets vertically grown on carbon fiber cloth for electrochemical capacitors. Journal of Alloys and Compounds 679, 277-284.
Ma, W., Meng, F., Cheng, Z., Sha, X., Xin, G., Tan, D., 2015. Synthesized of macroporous composite

electrode by activated carbon fiber and Mg–Ca–Al (NO3) hydrotalcite-like compounds to remove bromate. Colloids and Surfaces A: Physicochemical and Engineering Aspects 481, 393-399.

Ma, Y., Liu, D., Wu, H., Li, M., Ding, S., Hall, A.S., Xiao, C., 2021. Promoting Bifunctional Water Splitting by Modification of the Electronic Structure at the Interface of NiFe Layered Double Hydroxide and Ag. ACS Appl Mater Interfaces 13, 26055-26063.

Mahanta, A.K., Senapati, S., Paliwal, P., Krishnamurthy, S., Hemalatha, S., Maiti, P., 2019. Nanoparticle-Induced Controlled Drug Delivery Using Chitosan-Based Hydrogel and Scaffold: Application to Bone Regeneration. Molecular Pharmaceutics 16, 327-338.

Mai, W., Cui, Q., Zhang, Z., Zhang, K., Li, G., Tian, L., Hu, W., 2020. CoMoP/NiFe-Layered Double-Hydroxide Hierarchical Nanosheet Arrays Standing on Ni Foam for Efficient Overall Water Splitting. ACS Applied Energy Materials 3, 8075-8085.

Malafatti, J.O.D., Bernardo, M.P., Moreira, F.K.V., Ciol, H., Inada, N.M., Mattoso, L.H.C., Paris, E.C., 2020. Electrospun poly(lactic acid) nanofibers loaded with silver sulfadiazine/[Mg–Al]-layered double hydroxide as an antimicrobial wound dressing. Polymers for Advanced Technologies 31, 1377-1387.

Mandal, S., Mayadevi, S., 2008. Cellulose supported layered double hydroxides for the adsorption of fluoride from aqueous solution. Chemosphere 72, 995-998.

Manohara, G.V., 2014. Exfoliation of layered double hydroxides (LDHs): a new route to mineralize atmospheric CO2. RSC Adv. 4, 46126-46132.

Martin, J., Jack, M., Hakimian, A., Vaillancourt, N., Villemure, G., 2016. Electrodeposition of Ni-Al layered double hydroxide thin films having an inversed opal structure: Application as electrochromic coatings. Journal of Electroanalytical Chemistry 780, 217-224.

Martunus, Othman, M.R., Fernando, W.J.N., 2011. Elevated temperature carbon dioxide capture via reinforced metal hydrotalcite. Microporous and Mesoporous Materials 138, 110-117.

Meng, J., Yang, Z., Liu, L., Cui, F., Jiang, Y., 2019. The in-situ growth of zinc-aluminum hydrotalcite on hollow carbon spheres and its application as anode material with long cycle life for zinc-nickel secondary battery. Journal of Alloys and Compounds 809.

Miao, Y.-E., Zhu, H., Chen, D., Wang, R., Tjiu, W.W., Liu, T., 2012. Electrospun fibers of layered double hydroxide/biopolymer nanocomposites as effective drug delivery systems. Materials Chemistry and Physics 134, 623-630.

Mishra, G., Dash, B., Pandey, S., 2018. Layered double hydroxides: A brief review from fundamentals to application as evolving biomaterials. Applied Clay Science 153, 172-186.

Moriyama, S., Sasaki, K., Hirajima, T., 2016. Effect of freeze drying on characteristics of Mg–Al layered double hydroxides and bimetallic oxide synthesis and implications for fluoride sorption. Applied Clay Science 132-133, 460-467.

Mostajeran, M., Prévot, V., Mal, S.S., Mattiussi, E., Davis, B.R., Baker, R.T., 2017. Base-metal catalysts based on porous layered double hydroxides for alkaline-free sodium borohydride hydrolysis. International

Journal of Hydrogen Energy 42, 20092-20102.

Nadeema, A., Dhavale, V.M., Kurungot, S., 2017. NiZn double hydroxide nanosheet-anchored nitrogen-doped graphene enriched with the γ-NiOOH phase as an activity modulated water oxidation electrocatalyst. Nanoscale 9, 12590-12600.

Ni, X., Kuang, K., Jin, X., Xiao, X., Liao, G., 2010. Large scale synthesis of porous microspheres of Mg-Al-layerd double hydroxide with improved fire suppression effectiveness. Solid State Sciences 12, 546-551.

Ni, Y., Yao, L., Wang, Y., Liu, B., Cao, M., Hu, C., 2017. Construction of hierarchically porous graphitized carbon-supported NiFe layered double hydroxides with a core-shell structure as an enhanced electrocatalyst for the oxygen evolution reaction. Nanoscale 9, 11596-11604.

Nie, J., Hong, M., Zhang, X., Huang, J., Meng, Q., Du, C., Chen, J., 2020. 3D amorphous NiFe LDH nanosheets electrodeposited on: In situ grown NiCoP@NC on nickel foam for remarkably enhanced OER electrocatalytic performance. Dalton Transactions 49, 4896-4903.

Oestreicher, V., Jobbágy, M., 2013. One pot synthesis of Mg2Al(OH)6Cl·1.5H 2O layered double hydroxides: The epoxide route. Langmuir 29, 12104-12109.

Oka, Y., Kuroda, Y., Matsuno, T., Kamata, K., Wada, H., Shimojima, A., Kuroda, K., 2017. Preparation of Mesoporous Basic Oxides through Assembly of Monodispersed Mg–Al Layered Double Hydroxide Nanoparticles. Chemistry - A European Journal 23, 9362-9368.

Okada, K., Ricco, R., Tokudome, Y., Styles, M.J., Hill, A.J., Takahashi, M., Falcaro, P., 2014. Copper conversion into $Cu(OH)_2$ nanotubes for positioning Cu_3 $(BTC)_2$ MOF crystals: Controlling the growth on flat plates, 3D architectures, and as patterns. Advanced Functional Materials 24, 1969-1977.

Othman, M.R., Rasid, N.M., Fernando, W.J.N., 2006. Effects of thermal treatment on the micro-structures of co-precipitated and sol–gel synthesized (Mg–Al) hydrotalcites. Microporous and Mesoporous Materials 93, 23-28.

Pan, Z., Jiang, H., Gong, B., Luo, R., Zhang, W., Wang, G.-H., 2020. Layered double hydroxide derived NiAl-oxide hollow nanospheres for selective transfer hydrogenation with improved stability. Journal of Materials Chemistry A 8, 23376-23384.

Ping, J., Wang, Y., Lu, Q., Chen, B., Chen, J., Huang, Y., Ma, Q., Tan, C., Yang, J., Cao, X., Wang, Z., Wu, J., Ying, Y., Zhang, H., 2016. Self-Assembly of Single-Layer CoAl-Layered Double Hydroxide Nanosheets on 3D Graphene Network Used as Highly Efficient Electrocatalyst for Oxygen Evolution Reaction. Advanced Materials 28, 7640-7645.

Prevot, V., Caperaa, N., Taviot-Guého, C., Forano, C., 2009. Glycine-assisted hydrothermal synthesis of NiAl-layered double hydroxide nanostructures. Crystal Growth and Design 9, 3646-3654.

Prevot, V., Forano, C., Khenifi, A., Ballarin, B., Scavetta, E., Mousty, C., 2011a. A templated electrosynthesis of macroporous NiAl layered double hydroxides thin films. Chemical Communications 47, 1761-1763.

Prevot, V., Szczepaniak, C., Jaber, M., 2011b. Aerosol-assisted self-assembly of hybrid Layered Double Hydroxide particles into spherical architectures. Journal of Colloid and Interface Science 356, 566-572.

Prevot, V., Tokudome, Y., 2017. 3D hierarchical and porous layered double hydroxide structures: an overview of synthesis methods and applications. Journal of Materials Science 52, 11229-11250.

Prevot, V., Touati, S., Mousty, C., 2020. Confined Growth of NiAl-Layered Double Hydroxide Nanoparticles Within Alginate Gel: Influence on Electrochemical Properties. Frontiers in Chemistry 8.

Qin, M., Li, S., Zhao, Y., Lao, C.Y., Zhang, Z., Liu, L., Fang, F., Wu, H., Jia, B., Liu, Z., Wang, W.A., Liu, Y., Qu, X., 2019. Unprecedented Synthesis of Holey 2D Layered Double Hydroxide Nanomesh for Enhanced Oxygen Evolution. Advanced Energy Materials 9.

Qin, Q., Wang, J., Zhou, T., Zheng, Q., Huang, L., Zhang, Y., Lu, P., Umar, A., Louis, B., Wang, Q., 2017. Impact of organic interlayer anions on the CO_2 adsorption performance of Mg-Al layered double hydroxides derived mixed oxides. Journal of Energy Chemistry 26, 346-353.

Ray, S.S., Mosangi, D., Pillai, S., 2018. Layered Double Hydroxide-Based Functional Nanohybrids as Controlled Release Carriers of Pharmaceutically Active Ingredients. The Chemical Record 18, 913-927.

Reboul, J., Furukawa, S., Horike, N., Tsotsalas, M., Hirai, K., Uehara, H., Kondo, M., Louvain, N., Sakata, O., Kitagawa, S., 2012. Mesoscopic architectures of porous coordination polymers fabricated by pseudomorphic replication. Nature Materials 11, 717-723.

Rives, V., del Arco, M., Martín, C., 2014. Intercalation of drugs in layered double hydroxides and their controlled release: A review. Applied Clay Science 88-89, 239-269.

Romeo, V., Gorrasi, G., Vittoria, Chronakis, I.S., 2007. Encapsulation and Exfoliation of Inorganic Lamellar Fillers into Polycaprolactone by Electrospinning. Biomacromolecules 8, 3147-3152.

Sahoo, D.P., Patnaik, S., Parida, K., 2020. An amine functionalized ZnCr LDH/MCM-41 nanocomposite as efficient visible light induced photocatalyst for Cr(VI) reduction. Materials Today: Proceedings.

Sahoo, D.P., Patnaik, S., Rath, D., Mohapatra, P., Mohanty, A., Parida, K., 2019. Influence of Au/Pd alloy on an amine functionalised ZnCr LDH–MCM-41 nanocomposite: A visible light sensitive photocatalyst towards one-pot imine synthesis. Catalysis Science & Technology 9, 2493-2513.

Sailaja, G.S., Zhang, P., Anilkumar, G.M., Yamaguchi, T., 2015. Aniosotropically Organized LDH on PVDF: A Geometrically Templated Electrospun Substrate for Advanced Anion Conducting Membranes. ACS Applied Materials & Interfaces 7, 6397-6401.

Saliba, D., Ezzeddine, A., Sougrat, R., Khashab, N.M., Hmadeh, M., Al-Ghoul, M., 2016. Cadmium-Aluminum Layered Double Hydroxide Microspheres for Photocatalytic CO_2 Reduction. ChemSusChem 9, 800-805.

Shami, Z., Amininasab, S.M., Shakeri, P., 2016. Structure–Property Relationships of Nanosheeted 3D Hierarchical Roughness MgAl–Layered Double Hydroxide Branched to an Electrospun Porous Nanomembrane: A Superior Oil-Removing Nanofabric. ACS Applied Materials & Interfaces 8, 28964-28973.

Shao, M., Li, Z., Zhang, R., Ning, F., Wei, M., Evans, D.G., Duan, X., 2015. Hierarchical Conducting Polymer@Clay Core–Shell Arrays for Flexible All-Solid-State Supercapacitor Devices. Small 11, 3530-3538.

Shao, M., Ning, F., Zhao, J., Wei, M., Evans, D.G., Duan, X., 2013. Hierarchical layered double hydroxide microspheres with largely enhanced performance for ethanol electrooxidation. Advanced Functional Materials 23, 3513-3518.

Shao, M., Ning, F., Zhao, Y., Zhao, J., Wei, M., Evans, D.G., Duan, X., 2012. Core–Shell Layered Double Hydroxide Microspheres with Tunable Interior Architecture for Supercapacitors. Chemistry of Materials 24, 1192-1197.

Shi, Q., Huang, J., Yang, Y., Wu, J., Shen, J., Liu, X., Sun, A., Liu, Z., 2020a. In-situ construction of urchin-like hierarchical g-C3N4/NiAl-LDH hybrid for efficient photoreduction of CO_2. Materials Letters 268, 127560.

Shi, S., Zhang, W., Wu, H., Li, Y., Ren, X., Li, M., Liu, J., Sun, J., Yue, T., Wang, J., 2020b. In Situ Cascade Derivation toward a Hierarchical Layered Double Hydroxide Magnetic Absorbent for High-Performance Protein Separation. ACS Sustainable Chemistry & Engineering 8, 4966-4974.

Silva, L.C.P.B.B., Yun, A.E.H.K., Aguilera, C.S.B., Sousa, A.L.M.D., Melo, C.G., Timóteo, T.R.R., Danda, L.J.A., Oliveira, R.S., Silva, R.M.F., Rolim-Neto, P.J., 2019. Influence of drying processes on Layered Double Hydroxides as pharmaceutical excipients. Materials Letters 255.

Sobhana, S.S.L., Bogati, D.R., Reza, M., Gustafsson, J., Fardim, P., 2016. Cellulose biotemplates for layered double hydroxides networks. Microporous and Mesoporous Materials 225, 66-73.

Soler-Illia, G.J.D.A.A., Sanchez, C., Lebeau, B., Patarin, J., 2002. Chemical strategies to design textured materials: From microporous and mesoporous oxides to nanonetworks and hierarchical structures. Chemical Reviews 102, 4093-4138.

Song, S., Yu, L., Hadjiev, V.G., Zhang, W., Wang, D., Xiao, X., Chen, S., Zhang, Q., Ren, Z., 2019. New Way to Synthesize Robust and Porous $Ni_{1-x}Fe_x$ Layered Double Hydroxide for Efficient Electrocatalytic Oxygen Evolution. ACS Applied Materials and Interfaces 11, 32909-32916.

Song, Y., Wang, J., Li, Z., Guan, D., Mann, T., Liu, Q., Zhang, M., Liu, L., 2012. Self-assembled hierarchical porous layered double hydroxides by solvothermal method and their application for capacitors. Microporous and Mesoporous Materials 148, 159-165.

Sun, H., Chu, Z., Hong, D., Zhang, G., Xie, Y., Li, L., Shi, K., 2016. Three-dimensional hierarchical flower-like Mg-Al-layered double hydroxides: Fabrication, characterization and enhanced sensing properties to NO_x at room temperature. Journal of Alloys and Compounds 658, 561-568.

Sun, Q., Chen, B., 2020. Biotemplated Fabrication of 3D Hierarchically Porous MgAl-LDH/CF Composites with Effective Adsorption of Organic Dyes from Wastewater. Industrial & Engineering Chemistry Research 59, 16838-16850.

Sun, Y., Gao, X., Yang, N., Tantai, X., Xiao, X., Jiang, B., Zhang, L., 2019. Morphology-Controlled

Synthesis of Three-Dimensional Hierarchical Flowerlike Mg–Al Layered Double Hydroxides with Enhanced Catalytic Activity for Transesterification. Industrial & Engineering Chemistry Research 58, 7937-7947.

Suo, H., Duan, H., Chen, C., Buffet, J.-C., O'Hare, D., 2019. Bifunctional acid–base mesoporous silica@aqueous miscible organic-layered double hydroxides. RSC Advances 9, 3749-3754.

Taherian, Z., Shahed Gharahshiran, V., Khataee, A., Orooji, Y., 2021. Anti-coking freeze-dried NiMgAl catalysts for dry and steam reforming of methane. Journal of Industrial and Engineering Chemistry 103, 187-194.

Taherian, Z., Shahed Gharahshiran, V., Khataee, A., Orooji, Y., 2022. Synergistic effect of freeze-drying and promoters on the catalytic performance of Ni/MgAl layered double hydroxide. Fuel 311.

Tahir, M.U., Arshad, H., Zhang, H., Hou, Z., Wang, J., Yang, C., Su, X., 2020. Room temperature and aqueous synthesis of bimetallic ZIF derived CoNi layered double hydroxides and their applications in asymmetric supercapacitors. J Colloid Interface Sci 579, 195-204.

Takemoto, M., Tokudome, Y., Kikkawa, S., Teramura, K., Tanaka, T., Okada, K., Murata, H., Nakahira, A., Takahashi, M., 2020a. Imparting CO_2 reduction selectivity to $ZnGa_2O_4$ photocatalysts by crystallization from hetero nano assembly of amorphous-like metal hydroxides. RSC Advances 10, 8066-8073.

Takemoto, M., Tokudome, Y., Noguchi, D., Ueoka, R., Kanamori, K., Okada, K., Murata, H., Nakahira, A., Takahashi, M., 2020b. Synthesis of a Crystalline and Transparent Aerogel Composed of Ni-Al Layered Double Hydroxide Nanoparticles through Crystallization from Amorphous Hydrogel. Langmuir 36, 9436-9442.

Tammaro, L., Russo, G., Vittoria, V., 2009. Encapsulation of Diclofenac Molecules into Poly(ε-Caprolactone) Electrospun Fibers for Delivery Protection. J. Nanomater. 2009, 238206.

Tan, J.K.E., Balan, P., Birbilis, N., 2020. Advances in LDH coatings on Mg alloys for biomedical applications: A corrosion perspective. Applied Clay Science, 105948.

Tan, Y., Sun, D., Chen, L., Li, C.C., 2016. Porous Ru/RuO_X/LDH as highly active heterogeneous catalysts for the aerobic oxidation of alcohols. New Journal of Chemistry 40, 8364-8370.

Tang, Q., Angelomé, P.C., Soler-Illia, G.J.A.A., Müller, M., 2017. Formation of ordered mesostructured TiO_2 thin films: A soft coarse-grained simulation study. Physical Chemistry Chemical Physics 19, 28249-28262.

Tao, q., Xie, J., Li, Y., Dai, Y., Liu, Z., 2022. Effects of dry processing on adsorption of uranium on Mg-Al layered double hydroxides and calcined layered double oxides. Journal of Radioanalytical and Nuclear Chemistry 331, 4587-4600.

Tarutani, N., Tokudome, Y., Fukui, M., Nakanishi, K., Takahashi, M., 2015. Fabrication of hierarchically porous monolithic layered double hydroxide composites with tunable microcages for effective oxyanion adsorption. RSC Advances 5, 57187-57192.

Tarutani, N., Tokudome, Y., Jobbágy, M., Soler-Illia, G.J.A.A., Takahashi, M., 2019a. Mesoporous

microspheres of nickel-based layered hydroxides by aerosol-assisted self-assembly using crystalline nano-building blocks. Journal of Sol-Gel Science and Technology 89, 216-224.

Tarutani, N., Tokudome, Y., Jobbágy, M., Soler-Illia, G.J.A.A., Tang, Q., Müller, M., Takahashi, M., 2019b. Highly Ordered Mesoporous Hydroxide Thin Films through Self-Assembly of Size-Tailored Nanobuilding Blocks: A Theoretical-Experimental Approach. Chemistry of Materials 31, 322-330.

Tarutani, N., Tokudome, Y., Jobbágy, M., Viva, F.A., Soler-Illia, G.J.A.A., Takahashi, M., 2016. Single-Nanometer-Sized Low-Valence Metal Hydroxide Crystals: Synthesis via Epoxide-Mediated Alkalinization and Assembly toward Functional Mesoporous Materials. Chemistry of Materials 28, 5606-5610.

Tarutani, N., Tokudome, Y., Nakanishi, K., Takahashi, M., 2014. Layered double hydroxide composite monoliths with three-dimensional hierarchical channels: Structural control and adsorption behavior. RSC Advances 4, 16075-16080.

Taviot-Guého, C., Prévot, V., Forano, C., Renaudin, G., Mousty, C., Leroux, F., 2018. Tailoring Hybrid Layered Double Hydroxides for the Development of Innovative Applications. Advanced Functional Materials 28, 1703868.

Tian, N., Tian, X., Liu, X., Zhou, Z., Yang, C., Ma, L., Tian, C., Li, Y., Wang, Y., 2016a. Facile synthesis of hierarchical dendrite-like structure iron layered double hydroxide nanohybrids for effective arsenic removal. Chemical Communications 52, 11955-11958.

Tian, W., Kong, X., Jiang, M., Lei, X., Duan, X., 2016b. Hierarchical layered double hydroxide epitaxially grown on vermiculite for Cr(VI) removal. Materials Letters 175, 110-113.

Tokudome, Y., Fujita, K., Nakanishi, K., Miura, K., Hirao, K., 2007. Synthesis of monolithic Al_2O_3 with well-defined macropores and mesostructured skeletons via the sol-gel process accompanied by phase separation. Chemistry of Materials 19, 3393-3398.

Tokudome, Y., Fukui, M., Iguchi, S., Hasegawa, Y., Teramura, K., Tanaka, T., Takemoto, M., Katsura, R., Takahashi, M., 2018. A nanoLDH catalyst with high CO_2 adsorption capability for photo-catalytic reduction. Journal of Materials Chemistry A 6, 9684-9690.

Tokudome, Y., Fukui, M., Tarutani, N., Nishimura, S., Prevot, V., Forano, C., Poologasundarampillai, G., Lee, P.D., Takahashi, M., 2016a. High-Density Protein Loading on Hierarchically Porous Layered Double Hydroxide Composites with a Rational Mesostructure. Langmuir 32, 8826-8833.

Tokudome, Y., Morimoto, T., Tarutani, N., Vaz, P.D., Nunes, C.D., Prevot, V., Stenning, G.B.G., Takahashi, M., 2016b. Layered Double Hydroxide Nanoclusters: Aqueous, Concentrated, Stable, and Catalytically Active Colloids toward Green Chemistry. ACS Nano 10, 5550-5559.

Tokudome, Y., Poologasundarampillai, G., Tachibana, K., Murata, H., Naylor, A.J., Yoneyama, A., Nakahira, A., 2022. Curable Layered Double Hydroxide Nanoparticles- Based Perfusion Contrast Agents for X- Ray Computed Tomography Imaging of Vascular Structures. Advanced NanoBiomed Research 2, 2100123.

Tokudome, Y., Tarutani, N., Nakanishi, K., Takahashi, M., 2013. Layered double hydroxide (LDH)-based monolith with interconnected hierarchical channels: Enhanced sorption affinity for anionic species. Journal of Materials Chemistry A 1, 7702-7708.

Torchilin, V.P., 2007. Micellar nanocarriers: Pharmaceutical perspectives. Pharmaceutical Research 24, 1-16.

Touati, S., Mansouri, H., Bengueddach, A., De Roy, A., Forano, C., Prevot, V., 2012. Nanostructured layered double hydroxide aerogels with enhanced adsorption properties. Chemical Communications 48, 7197-7199.

Triantafyllidis, K.S., Peleka, E.N., Komvokis, V.G., Mavros, P.P., 2010. Iron-modified hydrotalcite-like materials as highly efficient phosphate sorbents. Journal of Colloid and Interface Science 342, 427-436.

Valarezo, E., Tammaro, L., González, S., Malagón, O., Vittoria, V., 2013. Fabrication and sustained release properties of poly(ε-caprolactone) electrospun fibers loaded with layered double hydroxide nanoparticles intercalated with amoxicillin. Applied Clay Science 72, 104-109.

Varga, G., Somosi, Z., Kónya, Z., Kukovecz, Á., Pálinkó, I., Szilagyi, I., 2021. A colloid chemistry route for the preparation of hierarchically ordered mesoporous layered double hydroxides using surfactants as sacrificial templates. Journal of Colloid and Interface Science 581, 928-938.

Vial, S., Prevot, V., Forano, C., 2006. Novel route for layered double hydroxides preparation by enzymatic decomposition of urea. Journal of Physics and Chemistry of Solids 67, 1048-1053.

Wan, H., Liu, J., Ruan, Y., Lv, L., Peng, L., Ji, X., Miao, L., Jiang, J., 2015. Hierarchical Configuration of $NiCo_2S_4$ Nanotube@Ni–Mn Layered Double Hydroxide Arrays/Three-Dimensional Graphene Sponge as Electrode Materials for High-Capacitance Supercapacitors. ACS Applied Materials & Interfaces 7, 15840-15847.

Wang, J., Mei, X., Huang, L., Zheng, Q., Qiao, Y., Zang, K., Mao, S., Yang, R., Zhang, Z., Gao, Y., Guo, Z., Huang, Z., Wang, Q., 2015. Synthesis of layered double hydroxides/graphene oxide nanocomposite as a novel high-temperature CO_2 adsorbent. Journal of Energy Chemistry 24, 127-137.

Wang, Q., Gao, Y., Luo, J., Zhong, Z., Borgna, A., Guo, Z., O'Hare, D., 2013. Synthesis of nano-sized spherical $Mg_3Al–CO_3$ layered double hydroxide as a high-temperature CO_2 adsorbent. RSC Advances 3.

Wang, Q., O'hare, D., 2013. Large-scale synthesis of highly dispersed layered double hydroxide powders containing delaminated single layer nanosheets. Chemical Communications 49, 6301-6303.

Wang, Y., Zhang, T., Xu, S., Wang, X., Evans, D.G., Duan, X., 2008. Preparation of layered-double hydroxide microspheres by spray drying. Industrial and Engineering Chemistry Research 47, 5746-5750.

Wong, M.S., Jeng, E.S., Ying, J.Y., 2001. Supramolecular Templating of Thermally Stable Crystalline Mesoporous Metal Oxides Using Nanoparticulate Precursors. Nano Letters 1, 637-642.

Woodford, J.J., Dacquin, J.-P., Wilson, K., Lee, A.F., 2012. Better by design: nanoengineered macroporous hydrotalcites for enhanced catalytic biodiesel production. Energy & Environmental Science 5.

Wu, L., Yu, L., Zhang, F., Wang, D., Luo, D., Song, S., Yuan, C., Karim, A., Chen, S., Ren, Z., 2020a. Facile synthesis of nanoparticle-stacked tungsten-doped nickel iron layered double hydroxide nanosheets for boosting oxygen evolution reaction. Journal of Materials Chemistry A 8, 8096-8103.

Wu, X., Jiang, L., Long, C., Wei, T., Fan, Z., 2015. Dual Support System Ensuring Porous Co-Al Hydroxide Nanosheets with Ultrahigh Rate Performance and High Energy Density for Supercapacitors. Advanced Functional Materials 25, 1648-1655.

Wu, Z., Khalafallah, D., Teng, C., Wang, X., Zou, Q., Chen, J., Zhi, M., Hong, Z., 2020b. Vanadium doped hierarchical porous nickel-cobalt layered double hydroxides nanosheet arrays for high-performance supercapacitor. Journal of Alloys and Compounds 838.

Xiao, Z., Mei, Y., Yuan, S., Mei, H., Xu, B., Bao, Y., Fan, L., Kang, W., Dai, F., Wang, R., Wang, L., Hu, S., Sun, D., Zhou, H.-C., 2019. Controlled Hydrolysis of Metal–Organic Frameworks: Hierarchical Ni/Co-Layered Double Hydroxide Microspheres for High-Performance Supercapacitors. ACS Nano 13, 7024-7030.

Xie, J., Yamaguchi, T., Oh, J.M., 2021. Synthesis of a mesoporous Mg–Al–mixed metal oxide with P123 template for effective removal of Congo red via aggregation-driven adsorption. Journal of Solid State Chemistry 293.

Xie, J., Zhang, X., Zhang, H., Zhang, J., Li, S., Wang, R., Pan, B., Xie, Y., 2017. Intralayered Ostwald Ripening to Ultrathin Nanomesh Catalyst with Robust Oxygen-Evolving Performance. Advanced Materials 29.

Xu, J., Deng, H., Song, J., Zhao, J., Zhang, L., Hou, W., 2017. Synthesis of hierarchical flower-like Mg_2Al-Cl layered double hydroxide in a surfactant-free reverse microemulsion. J Colloid Interface Sci 505, 816-823.

Xu, J., He, F., Gai, S., Zhang, S., Li, L., Yang, P., 2014. Nitrogen-enriched, double-shelled carbon/layered double hydroxide hollow microspheres for excellent electrochemical performance. Nanoscale 6, 10887-10895.

Xu, J., Zhao, Y., Li, M., Fan, G., Yang, L., Li, F., 2019. A strong coupled 2D metal-organic framework and ternary layered double hydroxide hierarchical nanocomposite as an excellent electrocatalyst for the oxygen evolution reaction. Electrochimica Acta 307, 275-284.

Xu, W., Mertens, M., Kenis, T., Derveaux, E., Adriaensens, P., Meynen, V., 2023. Can high temperature calcined Mg–Al layered double hydroxides (LDHs) fully rehydrate at room temperature in vapor or liquid condition? Materials Chemistry and Physics 295.

Xu, X., Cao, A., You, W., Tao, Z., Kang, L., Liu, J., 2021. Assembly of Cobalt Layered Double Hydroxide on Cuprous Phosphide Nanowire with Strong Built-In Potential for Accelerated Overall Water Splitting. Small 17, e2101725.

Xu, X., Zhong, Z., Yan, X., Kang, L., Yao, J., 2018. Cobalt layered double hydroxide nanosheets synthesized in water-methanol solution as oxygen evolution electrocatalysts. Journal of Materials

Chemistry A 6, 5999-6006.

Xu, Z.P., Stevenson, G.S., Lu, C.Q., Lu, G.Q., Bartlett, P.F., Gray, P.P., 2006. Stable suspension of layered double hydroxide nanoparticles in aqueous solution. J Am Chem Soc 128, 36-37.

Xue, L., Lü, Z., Cheng, Y., Sun, X., Lin, H., Xiao, X., Liu, X., Zhuo, S., 2018. Three-dimensional layered double hydroxide membranes: fabrication technique, growth mechanism, and enhanced photocatalytic activity. Chemical Communications 54, 8494-8497.

Yanagisawa, T., Shimizu, T., Kuroda, K., Kato, C., 1990. The preparation of alkyltrimethylammonium-kanemite complexes and their conversion to microporous materials. Bulletin of the Chemical Society of Japan 63, 988-992.

Yang, C., Wang, L., Yu, Y., Wu, P., Wang, F., Liu, S., Luo, X., 2020a. Highly efficient removal of amoxicillin from water by Mg-Al layered double hydroxide/cellulose nanocomposite beads synthesized through in-situ coprecipitation method. International Journal of Biological Macromolecules 149, 93-100.

Yang, C., Zhu, T., Wang, J., Chen, S., Li, W., 2015. Synthesis and characterization of flurbiprofen axetil-loaded electrospun MgAl-LDHs/poly(lactic-co-glycolic acid) composite nanofibers. RSC Advances 5, 69423-69429.

Yang, Q., Li, T., Lu, Z., Sun, X., Liu, J., 2014. Hierarchical construction of an ultrathin layered double hydroxide nanoarray for highly-efficient oxygen evolution reaction. Nanoscale 6, 11789-11794.

Yang, Y.J., Duan, M., Yan, C., Zhao, D., Jiang, C., Duan, X., Song, X., 2020b. Facile synthesis of CoFe-LDH/MWCNT/rGO nanocomposite as efficient bifunctional electrocatalysts for oxygen evolution and reduction. Journal of Electroanalytical Chemistry 856.

Yang, Z.-z., Wei, J.-j., Zeng, G.-m., Zhang, H.-q., Tan, X.-f., Ma, C., Li, X.-c., Li, Z.-h., Zhang, C., 2019. A review on strategies to LDH-based materials to improve adsorption capacity and photoreduction efficiency for CO_2. Coordination Chemistry Reviews 386, 154-182.

Yilmaz, G., Yam, K.M., Zhang, C., Fan, H.J., Ho, G.W., 2017. In Situ Transformation of MOFs into Layered Double Hydroxide Embedded Metal Sulfides for Improved Electrocatalytic and Supercapacitive Performance. Advanced Materials 29, 1606814.

Yin, S., Tu, W., Sheng, Y., Du, Y., Kraft, M., Borgna, A., Xu, R., 2018. A Highly Efficient Oxygen Evolution Catalyst Consisting of Interconnected Nickel–Iron-Layered Double Hydroxide and Carbon Nanodomains. Advanced Materials 30.

Yu, D., Wu, B., Ran, J., Ge, L., Wu, L., Wang, H., Xu, T., 2016a. An ordered ZIF-8-derived layered double hydroxide hollow nanoparticles-nanoflake array for high efficiency energy storage. Journal of Materials Chemistry A 4, 16953-16960.

Yu, J., Lu, L., Li, J., Song, P., 2016b. Biotemplated hierarchical porous-structure of ZnAl-LDH/$ZnCo_2O_4$ composites with enhanced adsorption and photocatalytic performance. RSC Advances 6, 12797-12808.

Yu, J., Wang, Q., O'Hare, D., Sun, L., 2017. Preparation of two dimensional layered double hydroxide nanosheets and their applications. Chemical Society Reviews 46, 5950-5974.

Yu, L., Yang, J.F., Guan, B.Y., Lu, Y., Lou, X.W.D., 2018. Hierarchical Hollow Nanoprisms Based on Ultrathin Ni-Fe Layered Double Hydroxide Nanosheets with Enhanced Electrocatalytic Activity towards Oxygen Evolution. Angewandte Chemie - International Edition 57, 172-176.

Yu, M., Wang, Z., Liu, J., Sun, F., Yang, P., Qiu, J., 2019. A hierarchically porous and hydrophilic 3D nickel–iron/MXene electrode for accelerating oxygen and hydrogen evolution at high current densities. Nano Energy 63, 103880.

Yu, X., Zhang, M., Yuan, W., Shi, G., 2015. A high-performance three-dimensional Ni-Fe layered double hydroxide/graphene electrode for water oxidation. Journal of Materials Chemistry A 3, 6921-6928.

Yu, X.Y., Luo, T., Jia, Y., Xu, R.X., Gao, C., Zhang, Y.X., Liu, J.H., Huang, X.J., 2012. Three-dimensional hierarchical flower-like Mg-Al-layered double hydroxides: highly efficient adsorbents for As(V) and Cr(VI) removal. Nanoscale 4, 3466-3474.

Yuan, X., Yin, C., Zhang, Y., Chen, Z., Xu, Y., Wang, J., 2019. Synthesis of C@Ni-Al LDH HSS for efficient U-entrapment from seawater. Sci Rep 9, 5807.

Yue, Y., Liu, F., Zhao, L., Zhang, L., Liu, Y., 2015. Loading oxide nano sheet supported Ni–Co alloy nanoparticles on the macroporous walls of monolithic alumina and their catalytic performance for ethanol steam reforming. International Journal of Hydrogen Energy 40, 7052-7063.

Zeng, S., Xu, X., Wang, S., Gong, Q., Liu, R., Yu, Y., 2013. Sand flower layered double hydroxides synthesized by co-precipitation for CO_2 capture: Morphology evolution mechanism, agitation effect and stability. Materials Chemistry and Physics 140, 159-167.

Zhan, T., Zhang, Y., Liu, X., Lu, S., Hou, W., 2016. NiFe layered double hydroxide/reduced graphene oxide nanohybrid as an efficient bifunctional electrocatalyst for oxygen evolution and reduction reactions. Journal of Power Sources 333, 53-60.

Zhang, B., Liu, W., Sun, D., Li, Y., Wu, T., 2019. Hollow nanoshell of layered double oxides for removal of 2,4-dichlorophenol from aqueous solution: Synthesis, characterization, and adsorption performance study. Colloids and Surfaces A: Physicochemical and Engineering Aspects 561, 244-253.

Zhang, C., Shao, M., Zhou, L., Li, Z., Xiao, K., Wei, M., 2016. Hierarchical NiFe Layered Double Hydroxide Hollow Microspheres with Highly-Efficient Behavior toward Oxygen Evolution Reaction. ACS Applied Materials and Interfaces 8, 33697-33703.

Zhang, F., Chen, J., Chen, P., Sun, Z., Xu, S., 2012. Pd nanoparticles supported on hydrotalcite-modified porous alumina spheres as selective hydrogenation catalyst. AIChE Journal 58, 1853-1861.

Zhang, F., Xie, Y., Xu, S., Zhao, X., Lei, X., 2010. Facile Fabrication and Magnetic Properties of Macroporous Spinel Microspheres from Layered Double Hydroxide Microsphere Precursor. Chemistry Letters 39, 588-590.

Zhang, H., Bai, Y., Chen, H., Wu, J., Li, C.M., Su, X., Zhang, L., 2022. Oxygen-defect-rich 3D porous cobalt-gallium layered double hydroxide for high-performance supercapacitor application. J Colloid Interface Sci 608, 1837-1845.

Zhang, J., Li, Z., Chen, Y., Gao, S., Lou, X.W.D., 2018a. Nickel–Iron Layered Double Hydroxide Hollow Polyhedrons as a Superior Sulfur Host for Lithium–Sulfur Batteries. Angewandte Chemie - International Edition 57, 10944-10948.

Zhang, J., Xie, X., Li, C., Wang, H., Wang, L., 2015. The role of soft colloidal templates in the shape evolution of flower-like MgAl-LDH hierarchical microstructures. RSC Advances 5, 29757-29765.

Zhang, L., Guo, D., Tantai, X., Jiang, B., Sun, Y., Yang, N., 2020a. Synthesis of Three-Dimensional Hierarchical Flower-Like Mg–Al Layered Double Hydroxides with Excellent Adsorption Performance for Organic Anionic Dyes. Transactions of Tianjin University.

Zhang, L., He, F., Mao, W., Guan, Y., 2020b. Fast and efficient removal of Cr(VI) to ppb level together with Cr(III) sequestration in water using layered double hydroxide interclated with diethyldithiocarbamate. Sci Total Environ 727, 138701.

Zhang, P., Wang, Z., Zhang, Y., Wang, J., Li, W., Li, L., Zhang, P., Wei, C., Miao, S., 2020c. Preparation of semi-hydrogenation catalysts by embedding Pd in layered double hydroxides nanocages via sacrificial template of ZIF-67. Applied Catalysis A: General 597, 117540.

Zhang, T., Mei, Z., Zhou, Y., Yu, S., Chen, Z., Bu, X., 2014. Novel paper-templated fabrication of hierarchically porous Ni-Al layered double hydroxides/Al_2O_3 for efficient BSA separation. Journal of Chemical Technology and Biotechnology 89, 1705-1711.

Zhang, Y., Ji, J., Li, H., Du, N., Song, S., Hou, W., 2018b. Synthesis of layered double hydroxide/poly(N-isopropylacrylamide) nanocomposite hydrogels with excellent mechanical and thermoresponsive performances. Soft Matter 14, 1789-1798.

Zhao, J., Chen, J., Xu, S., Shao, M., Zhang, Q., Wei, F., Ma, J., Wei, M., Evans, D.G., Duan, X., 2014. Hierarchical NiMn Layered Double Hydroxide/Carbon Nanotubes Architecture with Superb Energy Density for Flexible Supercapacitors. Advanced Functional Materials 24, 2938-2946.

Zhao, J., Lu, Z., Shao, M., Yan, D., Wei, M., Evans, D.G., Duan, X., 2013. Flexible hierarchical nanocomposites based on MnO_2 nanowires/CoAl hydrotalcite/carbon fibers for high-performance supercapacitors. RSC Advances 3, 1045-1049.

Zhao, J., Wang, X.R., Chen, F.W., He, C., Wang, X.J., Li, Y.P., Liu, R.H., Chen, X.M., Hao, Y.J., Yang, M., Li, F.T., 2020. A one-step synthesis of hierarchical porous CoFe-layered double hydroxide nanosheets with optimized composition for enhanced oxygen evolution electrocatalysis. Inorganic Chemistry Frontiers 7, 737-745.

Zhao, P., Liu, Y., Xiao, L., Deng, H., Du, Y., Shi, X., 2015a. Electrochemical deposition to construct a nature inspired multilayer chitosan/layered double hydroxides hybrid gel for stimuli responsive release of protein. Journal of Materials Chemistry B 3, 7577-7584.

Zhao, X., Zhang, L., Xiong, P., Ma, W., Qian, N., Lu, W., 2015b. A novel method for synthesis of Co–Al layered double hydroxides and their conversions to mesoporous $CoAl_2O_4$ nanostructures for applications in adsorption removal of fluoride ions. Microporous and Mesoporous Materials 201, 91-98.

Zheng, Y.-M., Li, N., Zhang, W.-D., 2012. Preparation of nanostructured microspheres of Zn–Mg–Al layered double hydroxides with high adsorption property. Colloids and Surfaces A: Physicochemical and Engineering Aspects 415, 195-201.

Zhou, J., Cheng, Y., Yu, J., Liu, G., 2011a. Hierarchically porous calcined lithium/aluminum layered double hydroxides: Facile synthesis and enhanced adsorption towards fluoride in water. Journal of Materials Chemistry 21, 19353-19361.

Zhou, J., Yang, S., Yu, J., Shu, Z., 2011b. Novel hollow microspheres of hierarchical zinc-aluminum layered double hydroxides and their enhanced adsorption capacity for phosphate in water. J Hazard Mater 192, 1114-1121.

Zhou, X., Mu, X., Cai, W., Wang, J., Chu, F., Xu, Z., Song, L., Xing, W., Hu, Y., 2019. Design of Hierarchical NiCo-LDH@PZS Hollow Dodecahedron Architecture and Application in High-Performance Epoxy Resin with Excellent Fire Safety. ACS Applied Materials & Interfaces 11, 41736-41749.

Zhu, J., Wang, Y., Ding, B., Dong, S., Dong, X., Dou, H., Zhang, X., 2019. Three-dimensional porous MXene-derived carbon/nickel-manganese double hydroxide composite for high-performance hybrid capacitor. Journal of Electroanalytical Chemistry 836, 118-124.

Zhu, L., Hao, C., Wang, X., Guo, Y., 2020. Fluffy Cotton-Like GO/Zn–Co–Ni Layered Double Hydroxides Form from a Sacrificed Template GO/ZIF-8 for High Performance Asymmetric Supercapacitors. ACS Sustainable Chemistry & Engineering 8, 11618-11629.

Zong, Y., Li, K., Tian, R., Lin, Y., Lu, C., 2018. Highly dispersed layered double oxide hollow spheres with sufficient active sites for adsorption of methyl blue. Nanoscale 10, 23191-23197.